

Improved Resistance to Thaumaside Formation in Cement Pastes by Early Age Carbonation

Alain Azar



Department of Civil Engineering and Applied Mechanics

McGill University

Montréal, Québec, Canada

May, 2013

A thesis submitted to McGill University in partial fulfillment of the requirements for
the degree of Master of Engineering

©Alain Azar, 2013

Abstract

Thaumasite formation in carbonated Ordinary Portland Cement (OPC) and carbonated Portland Limestone Cement (PLC) was investigated. The study was motivated by the question of whether or not the carbonation curing of concrete would make final concrete products more vulnerable to low temperature sulphate attack. The Thaumasite Form of Sulphate Attack (TSA) was discovered in concrete containing limestone powder exposed to sulphates in cold and damp environments. Carbonation curing of concrete could produce a large quantity of calcium carbonates in OPC and PLC, making them analogous to the concretes containing limestone powder. The vulnerability of carbonated concretes to thaumasite formation was thus studied. It was surprisingly found that carbonation curing at early age had significantly improved the resistance to TSA in both OPC and PLC. The improved resistance of carbonated cements was attributed to a decrease in pH at the surface of the specimens, a reduction in calcium hydroxide due to the carbonation reaction, the highly crystalline nature of calcium carbonates produced by carbonation, and the improved resistance to gas permeability.

Résumé

La formation de thaumasite dans du ciment Portland ordinaire et du ciment Portland comportant du carbonate de calcium qui furent sujet à la carbonatation fut vérifiée. La motivation de la recherche est de déterminer si le béton carboné est vulnérable à une attaque chimique en présence de sulfates, lorsque exposé à de basses températures. La formation de thaumasite fut remarquée dans du béton contenant du ciment Portland comportant du carbonate de calcium. La carbonatation du béton produit aussi une grande quantité de carbonate de calcium, ce qui peut rendre ce type de béton plus vulnérable à la formation de thaumasite. La vulnérabilité du béton sujet à la carbonatation et exposé au thaumasite fut donc étudiée. Il fut surprenant de trouver que le béton sujet à la carbonatation avait une résistance améliorée à la formation de thaumasite. L'amélioration de la résistance du béton carboné fut attribuée à une réduction du pH à la surface des spécimens, une diminution de l'hydroxyde de calcium présent dans le ciment due à la réaction de carbonatation, la structure cristalline des carbonates formés par carbonatation, et la nature moins perméable des spécimens sujets à la carbonatation.

Acknowledgements

First and foremost, I would like to thank my supervisor, Professor Yixin Shao, for his priceless guidance and support throughout the thesis. His experience was absolutely crucial throughout the thesis. The support by the Natural Science and Engineering Research Council (NSERC) of Canada and Canadian Concrete Masonry Producers Association (CCMPA) is gratefully acknowledged. I would also like to thank Professor Andrew Boyd. His knowledge with regards to sulphate attack in concrete was extremely useful and the guidance he provided greatly appreciated.

I would like to express my gratitude to my colleagues, Hilal El-Hassan, Zaid Ghoulleh, Lana Tayara, Vahid Rostami, Mehrdad Mahoutian, Yaodong Jia, Abu Morshed and Erwan Lerigoleur, for their support. Special thanks to John Bartczak for his help with the modified surface permeability chamber. Also, I would like to thank Gul Zeb for the precious help generating the Raman spectra, and Saikat Chatterjee for the help with TGA experiments. I would also like to thank Samantha Walker for her precious help and encouragements.

Many thanks go out to my parents, Charles and Maha, as well as my brother Simon, without whose support I would not be where I am today. Finally, thanks to all my friends that stood by my side throughout these busy years.

Table of Contents

Abstract.....	ii
Résumé.....	iii
Acknowledgements.....	iv
List of Figures.....	vii
List of Tables.....	ix
Chapter 1: Introduction.....	1
Chapter 2: Literature Review.....	4
2.1 Sulphate attack at ambient temperatures.....	4
2.2 Thaumasite form of sulphate attack at low temperatures.....	8
2.3 Test methods for sulphate attack at ambient and low temperatures.....	12
2.3.1 Standard test methods.....	12
2.3.2 Non-standard test methods.....	14
2.4 Carbonation curing of cement and concrete.....	15
2.5 Research objectives.....	17
Chapter 3: Experimental Program.....	18
3.1 Preparation of specimens.....	18
3.1.1 Materials.....	19
3.1.2 Mixing and casting procedures.....	19
3.1.3 Carbon dioxide curing and uptake.....	22
3.2 Sulphate exposure conditions.....	24
3.3 Testing.....	26
3.3.1 Visual assessment.....	28
3.3.2 Compressive strength.....	28
3.3.3 Change in mass.....	30
3.3.4 Change in length.....	31
3.3.5 X-Ray Diffraction (XRD).....	33
3.3.6 Thermogravimetric analysis and differential thermal analysis.....	33
3.3.7 Raman spectroscopy.....	34
3.3.8 Surface air permeability.....	34
3.3.9: pH measurements.....	36

Chapter 4: Results and Discussions	38
4.1 Early carbonation curing of cement pastes and mortar bars	38
4.1.1 Carbonation curing and CO ₂ uptake	39
4.1.2 Phase analysis by x-ray diffraction	42
4.1.3 Compressive strength	43
4.2 Thaumasite formation in hydrated and carbonated OPC and PLC	45
4.2.1 Visual inspection	45
4.2.2 Mass loss	50
4.2.3 Compressive strength	53
4.2.4 Change in length	55
4.3 Effect of thaumasite form of sulphate attack on mineralogy of cement paste	58
4.3.1 X-ray diffraction	58
4.3.2 Thermogravimetric Analysis (TGA) and Differential Thermal Analysis (DTA)	66
4.3.3 Raman spectroscopy	71
4.4 Mechanism of sulphate resistance by early age carbonation	75
4.4.1 Surface air permeability	76
4.4.2 Crystalline nature of produced carbonates	78
4.4.3 pH measurements	79
4.4.4 Calcium hydroxide content	82
Chapter 5: Conclusions	84
References	88

List of Figures

Figure 2-1: Summary of ESA related issues (Skalny et. al 2002, p. 106).....	6
Figure 3-1: Carbonation setup.....	23
Figure 3-2: Low temperature sulphate attack test setup	25
Figure 3-3: MTS Sintech	29
Figure 3-4: Compression strength tests	30
Figure 3-5: Change in length of mortar bar measurements.....	32
Figure 3-6: Surface air permeability test apparatus.....	35
Figure 3-7: Surface air permeability test setup.....	36
Figure 4-1: XRD patterns of pastes after 28 days of curing	43
Figure 4-2: Compressive strength of cement pastes after 28 hours and 28 days of curing	44
Figure 4-3: Cement paste cubes after submerged in a 5% MgSO ₄ solution for 6 months at 5°C	47
Figure 4-4: Cement paste cubes after submerged in a 5% MgSO ₄ solution for 10 months at 5°C	49
Figure 4-5: Mass change of cement paste cubes versus time Mass change of cement paste cubes versus time.....	50
Figure 4-6: Mass change of cement paste cubes.....	52
Figure 4-7: Compressive Strength of Cement Paste Specimens	53
Figure 4-8: Expansion of mortar bars.....	56
Figure 4-9: Mortar bars following 10 months of exposure to MgSO ₄ at 5°C.....	57
Figure 4-10: XRD patterns of ettringite (E) and thaumasite (T) (hartshorn et al., 1999).....	59
Figure 4-11: XRD pattern of Gypsum.....	59
Figure 4-12: XRD pattern of hydrated OPC specimens	60
Figure 4-13: XRD patterns of carbonated OPC specimens.....	61
Figure 4-14: XRD patterns of hydrated PLC specimens	62
Figure 4-15: XRD patterns of spalled and core of hydrated PLC specimen	63
Figure 4-16: XRD patterns of carbonated PLC specimens	65
Figure 4-17: DTA of cement pastes at 10 months of MgSO ₄ exposure.....	68
Figure 4-18: DTG of cement pastes at 10 months of MgSO ₄ exposure	69
Figure 4-19: Quantitative TG analysis of cement paste at 10 months of MgSO ₄ exposure	70
Figure 4-20: Raman spectra of thaumasite, ettringite and gypsum (Sadananda et. al. 2002).....	72
Figure 4-21: Raman spectra of cement paste cubes exposed to sulphate attack for 10 months at 5°C	73
Figure 4-22: Surface air permeability of cement paste specimens.....	77
Figure 4-23: pH of cement paste cubes	80

Figure 4-24: Phenolphthalein photographs at the outer surface (a) and cross-section (b) of specimens 82

List of Tables

Table 2-1: Exposure classes specified in ACI 318:2008	13
Table 2-2: Expansion limits when using ASTM C1012 (ACI 318:2008)	14
Table 3-1: Chemical composition of the cements.....	19
Table 3-2: Curing regimes.....	21
Table 3-3: Environmental conditions during mixing and open air curing	22
Table 3-4: Tests performed on pastes and mortars	27
Table 3-5: Deviations between current research and ASTM C 1012	31
Table 4-1: Water content change during carbonation curing.....	39
Table 4-2: CO ₂ uptake of cement paste and mortar	40
Table 4-3: Equivalent CaCO ₃ content of cement pastes	41
Table 4-4: Morphology of CaCO ₃ in cement pastes	78

Chapter 1: Introduction

The use of limestone as a component of Portland cement has become very widespread in Canada and world over. In Canada, the Canadian Standards Association (CSA) allows the inclusion of up to 5% limestone addition in Ordinary Portland Cement (OPC), and 15% limestone addition in Portland Limestone Cement (PLC). Since recently, the American Society for Testing and Materials (ASTM) C595 standard also permits the use of 15% limestone addition by cement mass in PLC. The European standard, EN 197-1, permits the common cement products to contain up to 5% limestone. In addition, EN 197-1 covers PLC, which may contain up to 35% limestone addition. Many Latin American country standards also allow PLC with up to 35% limestone addition. Therefore, the production of Portland Limestone Cement (PLC) has increased in the past decades. The increased interest and production of PLC is explained by the technical, economical and environmental benefits (Tennis et al. 2011). It is promoted by the sustainable development in cement industry to use less clinker and reduce energy and its related emissions. Indeed, the performance of PLC has been reported comparable to that of OPC except in a special condition: the service temperature of concrete is below 15°C, and in the presence of rich sulphate environments. This typically happens in cases where the concrete is exposed to groundwater at low temperatures. The reaction product of the deterioration is called thaumasite.

Thaumasite is a natural mineral. It is in fact a modified form of ettringite. Thaumasite is formed in the presence of calcium silicate, sulphate and carbonate ions. The occurrence of thaumasite is more favorable at low temperatures. The Thaumasite form of Sulphate Attack (TSA) is detrimental in that it destroys the binding ability of the concrete. TSA transforms concrete into a non-cohesive mass or mush by attacking the binding ability of the Calcium-Silicate-Hydrates (CSH). In the presence of abundant amounts of carbonates and sulphates, TSA is in principle unlimited until all the calcium silicate from the CSH is consumed. It is the reason that PLC is not allowed in sulphate-containing environments.

Limestone can be one source of carbonates for thaumasite to form in concrete exposed to sulphates. There are other mechanisms that introduce calcium carbonates in concrete. One of these processes is called early age carbonation curing, which has received renewed interests because of its potential to recycle carbon dioxide from cement production, by converting gaseous carbon dioxide into solid carbonates within the concrete. The process also accelerates hydration and improves durability (Shao et al. 2006). However the process also increases the calcium carbonate content in concrete, making carbonated OPC concrete similar to PLC concrete. As far as the chemical composition is concerned, both PLC and carbonated concretes contain large quantities of calcium carbonates. The problem facing PLC concrete could be the same for concrete subjected to early carbonation, due to the carbonate content. Carbonated concrete could be especially vulnerable when the degree of carbonation is high, where the CaCO_3 content in concrete will be increased

considerably. Therefore, it is imperative to know if the carbonated concrete is also vulnerable to sulfate attack at low temperatures due to the formation of thaumasite.

Chapter 2: Literature Review

This chapter introduces past research and the theory of sulphate attack on concrete, with a special focus on TSA. The first section of this chapter presents the theory behind conventional sulphate attack in concrete at ambient temperatures, where the formation of ettringite in hardened concrete causes the damage to concrete. The second section explains the formation of thaumasite and TSA. The literature done to date on concrete containing limestone filler deteriorated by TSA is also presented. The third portion details existing test methods to determine the vulnerability of concrete to conventional sulphate attack and TSA. The fourth section presents early age carbonation curing of concrete. The research objectives are summarized in the last section of Chapter 2.

2.1 Sulphate attack at ambient temperatures

The term sulphate attack refers to a series of chemical reactions between the components of the hydrated cement paste of a concrete sample and a form of sulphate. The reactions are caused by exposure of concrete to moisture and sulphates (Skalny et al. 2002, p.43). As it represents a complex set of chemical and physical processes, it cannot be fully characterized by a single mechanism (Skalny and Pierce, 1999). Neville (2004) adds that the term sulphate attack may only be used if there is damage and deterioration of the concrete. Therefore, the presence alone of certain compounds that can cause sulphate attack, such as ettringite and thaumasite, without actual damage, does not refer to sulphate

attack. The formation of thaumasite is therefore only referred to as TSA in the presence of damage. As well, the outcome of the deterioration is related to several elements such as temperature, solution concentration and exposure. Skalny et al. (2002) emphasise that the chemistry of sulphate attack is independent of the source of sulphate. Instead, it is governed by environmental and physical conditions under which the reactions proceed.

External Sulphate Attack (ESA) is induced by a source of sulphates that is exterior to concrete. ESA induced damage will occur if there is a sulphate rich environment, permeable concrete and with the presence of water (Collepardi 2003). Damage from ESA includes excessive expansion, crack formation, surface spalling, delamination and loss of strength. The chemical process involved in External Sulphate Attack is strongly linked to the type of sulphate involved in the reaction. Once the sulphates enter the concrete from an outside source, by means of several transport mechanisms, one of three chemical processes can occur depending on the predominant reaction. These processes lead to the formation of gypsum, ettringite or thaumasite, when exposed at low temperatures (Collepardi 2003). A summary of ESA related issues is shown in Figure 2-1 below.

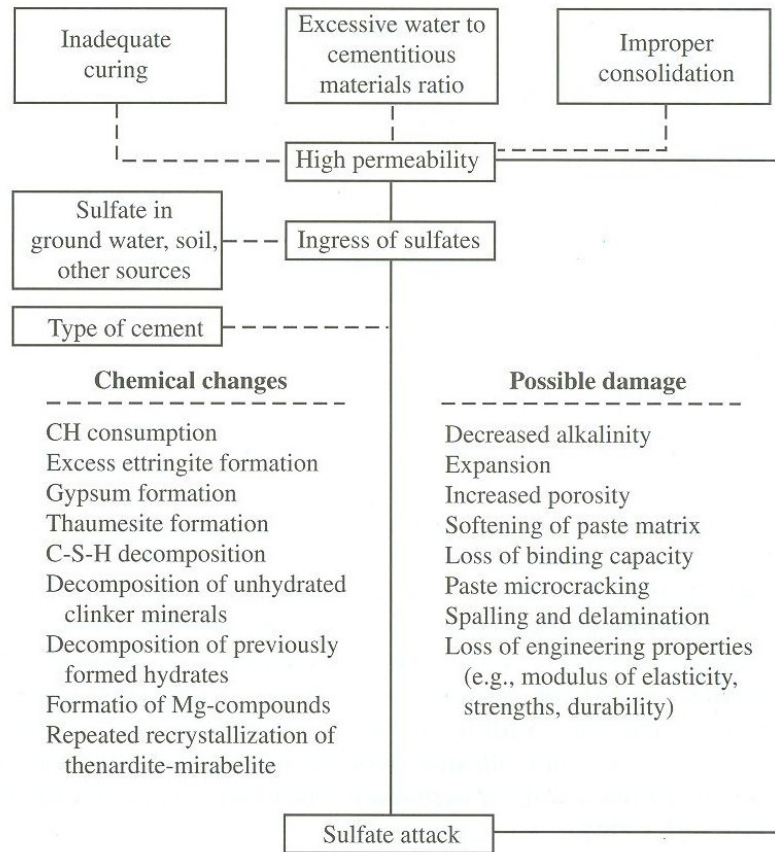
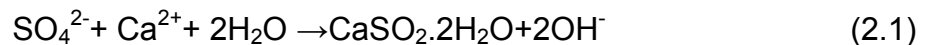


Figure 2-1: Summary of ESA related issues (Skalny et. al 2002, p. 106)

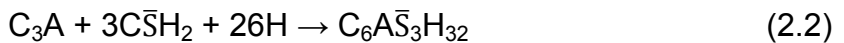
The process involving the formation of gypsum occurs when the sulphates react with calcium hydroxide. The type and source of sulphate affect the quantity of gypsum produced. This reaction is referred to as gypsum corrosion (Santhanam et al. 2003):



The formation of gypsum may cause expansion but usually leads to cracking and spalling. However, due to the round shape of gypsum, the most

important feature of gypsum corrosion is the loss of strength and adhesion of the cement paste due to the de-calcification of CSH (Tian and Cohen, 2000).

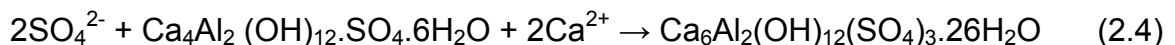
The second possible outcome of ESA involves the formation of ettringite. Early ettringite formed within hours of the contact between cement and water is not detrimental to concrete as the mix remains in the plastic state. In this reaction, ettringite precipitates at the surface of C₃A when this compound reacts with gypsum (Harthsorn et al. 1999):



This ettringite is then converted to the Afm phase, or calcium aluminate monosulphate hydrates (Hewlett 2004, p.261):



However, in the presence of sodium sulphate ions, the sulphate ions enter the concrete and react with monosulphate compounds formed from equation 2.3 to form ettringite (skalny et al. 2002, p.93):



If the ettringite is formed in the later stages of hydration, after the concrete hardens, it will cause cracking upon expansion due to its shape. The so called delayed ettringite formation will result in expansion related cracking (Colleparidi 2003).

The main component of cement involved in the intensity of conventional sulphate attack is C₃A. Improving the transport properties of concrete is also an

effective measure to prevent ESA. This reduction in flow through concrete can be achieved by reducing the water-cement ratio.

The third possible manifestation of ESA-related damage occurs when there is sulphate attack on CSH and Calcium Hydroxide in the presence of carbonate ions to form thaumasite, and occurs at low temperatures. This reaction is reviewed in section 2.2.

In the presence of a magnesium sulphate solution, the reaction results in the formation of conventional sulphate attack products (ettringite and gypsum) but also results in the formation of calcium sulphate in the form of gypsum, and magnesium hydroxyde (skalny et al. 2002, p.98):



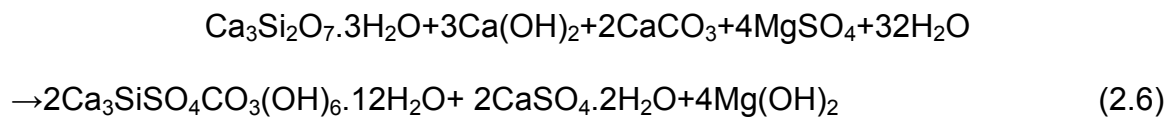
During and following the reaction with calcium hydroxide, magnesium sulphate attack leads to the decomposition of the CSH. This degradation is faster and more thorough than with other sulphate compounds due to the low pH of the solution and the low solubility of magnesium hydroxide (Skalny et al. 2002, p.99).

2.2 Thaumasite form of sulphate attack at low temperatures

A report recently published by the UK Government's Thaumasite Expert Group highlighted the identification of thaumasite as a product of sulphate attack of columns supporting bridges, in which the concrete contained limestone filler (Crammond 2003). Many studies have been conducted to determine the susceptibility of PLC cement to thaumasite formation. Most experiments showed

that the rate of thaumasite formation strongly increased with increasing limestone content (Kakali et al. 2003, Tsvivilis et al. 2007, Torres et al. 2004).

Thaumasite may be formed when carbonate and calcium silicate ions are present in the pore solution of cement paste at low temperatures (Irassar 2009). TSA takes place in the presence of sulphate-bearing groundwater. This reaction is shown below (Skalny et al. 2002, p.103):



From equation 2.6, it is seen that the reactants for the formation of thaumasite are CSH and calcium hydroxide from cement hydration, carbonates that can be from multiple sources such as limestone filler and aggregates, sulphates and water. The reaction products of equation 2.6 are thaumasite, gypsum and brucite.

Unlike traditional sulphate attack, where the amount of ettringite that can form is limited by the alumina content of the cement, TSA damage is in principle unlimited. Indeed, thaumasite can be formed as long as external sulphates and carbonate ions are provided, and its formation is not limited by the alumina content of the cement. The needed silica is taken from the CSH and the reaction can proceed indefinitely until all the CSH is gone. Carbonate ions usually originate from carbonate rocks constituting the concrete aggregates, calcium carbonate inter-ground with the cement or groundwater with high amounts of dissolved CO_2 (Skalny et al. 2002). Concrete containing limestone (CO_3^{2-}) as

filler and exposed to a sulphate solution is also particularly vulnerable to Thaumaside Sulphate Attack (TSA) as mentioned above. The threshold amount of carbonates in an aggregate needed to initiate thaumasite formation and TSA depends on the fineness of the particles. Concrete mixes that contain finely divided calcium carbonate are predominantly susceptible to the formation of thaumasite (Skalny et al. 2002, p.104).

TSA is accompanied by the most severe loss of strength. This type of sulphate attack causes a gradual softening of the surface of concrete as well as a gradual inwards progression until the cement paste is transformed into a non-cohesive mass leading to the loss of particles (Crammond 2003). TSA-related deterioration can be more damaging than conventional forms of sulphate attacks as it is associated with the deterioration of the CSH gel. This deterioration is a result of the reaction of thaumasite that uses silicate ions from the CSH.

In terms of chemistry, thaumasite is a modified form of ettringite, or an AFt compound. Thaumasite is structurally similar to ettringite, with $\text{Si}(\text{OH})_6^{2-}$ in the place of $\text{Al}(\text{OH})_6^{3-}$ and $(2\text{CO}_3^{2-} + 2\text{SO}_4^{2-})$ instead of $(3\text{SO}_4^{2-} + 2\text{H}_2\text{O})$ (Skalny et al. 2002). However, unlike ettringite, it is not a natural hydration product. Most researchers make use of X-ray Diffraction (XRD) to identify thaumasite. Thaumasite can be identified based on peaks at around 16, 23.5 and 28° 2 θ , which are not present in the ettringite pattern. The absence of ettringite can also be confirmed by the absence of its characteristic peaks at around 15.8, 18.9, 22.9, 25.5° 2 θ (Kakali et al. 2003).

The general conditions for thaumasite formation are a source of calcium silicate, carbonate and sulphate ions, excess water and low temperatures. Low temperatures are favorable for the formation of thaumasite as the solubility of carbonates is increased, and thaumasite is more insoluble at cold temperatures (Crammond 2003). Irassar (2009) combines the factors of thaumasite formation in three categories: the composition of mixtures, characteristics of cementitious materials and aggressiveness of sulphate environment. It has also been found that a high pH pore solution at the concrete surface exposed to sulphates will encourage the onset of TSA. Indeed, Crammond (2003) notes that TSA will continue forming as long as necessary ions are supplied, and the reaction front is kept at cold temperatures, and maintained at a high pH.

Another theory on the mechanism of thaumasite suggests that there is a “possible topochemical replacement of ettringite by thaumasite” (Crammond 2003). Indeed, it has been suggested that when a small amount of alumina is present among the reactants, the synthesis of thaumasite is encouraged, which is commonly associated to the fact that ettringite is a precursor to the formation of thaumasite. The fact that they both have similar structures suggest that a solid solutions series between the two minerals is possible, where there would be a “topochemical interchange of (Si) for (Al) and $(\text{CO}_3^{2-} + \text{SO}_4^{2-})$ and $(\text{SO}_4^{2-} + \text{H}_2\text{O})$ ” (Crammond 2003). However, in TSA, thaumasite forms continuously throughout the paste, not only in areas where ettringite is present (Crammond 2003).

Thaumasite formation can also be strongly dictated by the sulphate solution present. As mentioned above, TSA induced by magnesium sulphate

compounds will be more severe. It has been found that TSA can be formed from magnesium sulphate and sodium sulphate at high concentrations. Magnesium sulphate has also been shown to be more detrimental to concrete in general as mentioned previously (Hartshorn et al. 1999). Although both solutions are neutral, their respective evolution in pH is different. The pH in a sodium solution increases rapidly to approximately 12 where magnesium solutions may be buffered at a pH near 7 (Irassar 2009).

Finally, it should be noted that the permeability of concrete plays an important role in the formation of thaumasite. The formation of thaumasite requires sulphate ions, which need to enter the concrete to react. Therefore, improving transport properties of concrete contributes to improving the resistance of concrete to thaumasite.

2.3 Test methods for sulphate attack at ambient and low temperatures

The standard and non standard test methods to determine the vulnerability of concrete to sulphate attack are presented hereafter. ASTM Standards used for this purpose are presented and discussed in section 2.3.1. Other relevant test methods used by researchers to identify and quantify TSA are presented in section 2.3.2.

2.3.1 Standard test methods

The standard test methods for sulphate attack are presented hereafter. Their limitations are also discussed below.

- ASTM C 452: Standard Test Method for Potential Expansion of Portland-Cement Mortars Exposed to Sulfate Solution
- ASTM C1012: Standard Test Method for Length Change of Hydraulic-Cement Mortars Exposed to a Sulfate Solution

ASTM C 452 is used for internal sulphate attack. The ASTM C1012, which is used for external sulphate attack, prescribes a method to monitor the change in length of mortar bars exposed to a 5% sulphate solution at $23.0 \pm 2.0^{\circ}\text{C}$. All damage is reported in terms of expansion. The exposure classes are defined in Table 2-1, and expansion limits corresponding to different exposure classes are shown in Table 2-2.

Table 2-1: Exposure classes specified in ACI 318:2008

S Sulfate	SO (Not applicable)	SO ₄ < 0.10% (soil) SO ₄ < 150 ppm (water)
	S1 (moderate)	0.10 ≤ SO ₄ < 0.20% (soil) 150 ≤ SO ₄ < 1500 ppm (water)
	S2 (severe)	0.20 ≤ SO ₄ < 2.00% (soil) 1500 ≤ SO ₄ < 1000 ppm (water)
	S3 (very severe)	SO ₄ > 2.00% (soil) SO ₄ > 10000 ppm (water)

Table 2-2: Expansion limits when using ASTM C1012 (ACI 318:2008)

Exposure Class	Maximum expansion when tested using ASTM C 1012
S1	0.10 % at 6 months
S2	0.05 percent at 6 months or 0.10% at 12 months
S3	0.10% at 18 months

It should be noted that TSA leads to the decalcification of the CSH matrix, in turn leading to paste softening. Therefore, ASTM standards presented above are not representative of TSA-induced damage. Indeed, as mentioned previously, TSA damage would not necessarily result in concrete expansion. Instead, the concrete would suffer from loss of cohesion. As well, these standards do not prescribe storing samples at low temperatures. Another limitation of these standards is the fact that neither standard addresses the effect of sulphate attack on mechanical properties of concrete. Due to these limitations, these standard procedures should not be used alone to monitor TSA-induced damage on concrete.

2.3.2 Non-standard test methods

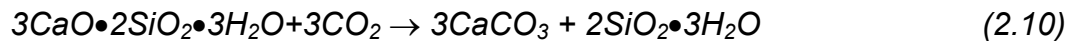
In most studies that monitor sulphate attack at low temperatures and TSA, the specimens are stored at approximately 5°C to encourage the formation of thaumasite (Hartshorn et al. 1999, Kakali et al. 2003, Torres et al. 2004, Tsvilis et al. 2007). These experiments are conducted using different mixtures with varying water-cement ratios and limestone content. Generally, X-ray diffraction (XRD) is used to determine the presence of thaumasite and effectively

differentiate ettringite and thaumasite. Differential thermal analysis (DTA) has also been used for this purpose (Kakali et al. 2003). Finally, the mineralogical composition of affected specimens has also been analysed using Raman spectroscopy (Sadananda et al. 2002). Other indicators are used in these studies to monitor TSA-induced damage, such as change in mass of concrete specimens throughout exposure, compressive strength and visual inspections (Kakali et al. 2003, Tsivilis et al. 2007).

2.4 Carbonation curing of cement and concrete

With the alarming increase in Carbon dioxide (CO₂) emissions over the past five decades, specific ways to reduce these emissions must urgently be sought out. An additional challenge arises from determining methods that beneficially utilize the captured CO₂ in commercial production, thus avoiding underground geological storage. Early age carbonation curing of concrete is an effective measure to sequester recovered CO₂ in lime or cement-based products. With the use of this method, CO₂ is beneficially utilized to improve early age strength and enhance the late age durability performance with more resistance to permeation, dimension change and freeze-thaw damage. In a CO₂ cap and trade system, concrete producers can even claim carbon credits through early carbonation. Cap and trade markets are already gaining importance all over the world. Such a system is already widespread in Europe and beginning to emerge in North-America. The approach can show technical, economical and environmental benefits.

In this process, CO₂ is injected into a chamber at room temperature. The carbon dioxide then diffuses into fresh concrete under low pressure and transforms the gaseous CO₂ in solid calcium carbonates (CaCO₃) through the reactions shown below:



This CO₂ consuming process is best suited for pre-cast concrete units such as masonry units, pipes and footings. Pre-cast concrete units are suitable as they are also cured in chambers, traditionally using steam.

By carbonation curing, it has been found that cement paste can have a CO₂ uptake of approximately 7-8% (Rostami et al. 2012). This carbon dioxide uptake results in a calcium carbonate uptake of 16-18% through the carbonation reaction. Therefore, it should be noted that carbonated OPC is actually similar to PLC in terms of carbonate content, although the carbonates differ in size. Also, carbonated PLC actually contains almost double of the carbonate content in PLC. Knowing the vulnerability of PLC due to carbonate ions from limestone filler, this research was motivated by the question of whether or not the carbonation curing of concrete would make final concrete products more vulnerable to the thaumasite form of sulphate attack.

2.5 Research objectives

Since PLC concrete has shown vulnerability to TSA, it is imperative to determine if carbonated concrete is also vulnerable to this form of sulphate attack due to the formation of calcium carbonates. Therefore, the research objectives of this thesis were to perform early age carbonation curing of OPC and PLC pastes, to study the thaumasite formation in carbonated OPC and PLC pastes, and to understand the effect of early age carbonation curing on TSA.

In order to reach the research objectives, paste and mortar specimens were prepared, and half of the specimens carbonated and half hydrated as references. Following 28 days of subsequent hydration, the specimens were subject to conditions favorable to TSA: the presence of sulphate ions and low temperatures. These specimens were then monitored throughout the exposure for various deterioration indicators including change in mass, compressive strength and change in length. Mineralogical composition was also evaluated using XRD, Thermogravimetric analysis (TGA) and Raman spectroscopy to assess the effect of TSA on specimens. Hydrated specimens were used as reference, and it was therefore possible to evaluate the degree of resistance of carbonated cements to TSA.

Chapter 3: Experimental Program

This chapter outlines the experimental program that was designed to examine the effect of early age carbonation curing on the concrete resistance to thaumasite formation. The first section focuses on the preparation of specimens including the materials used, mixing and casting procedures, and the carbonation process. Furthermore, the experiments conducted to determine the carbon dioxide uptake are described. The second section highlights the sulphate exposure conditions to which the specimens were subject. The third section describes all the experiments that were conducted to evaluate the performance of cement paste specimens at different exposure conditions.

3.1 Preparation of specimens

To eliminate the influence of aggregates on the thaumasite formation and examine the effect of early carbonation-induced carbonates on the thaumasite form sulphate attack, mainly cement paste was used, instead of concrete, in preparing the specimens. Both ordinary Portland cement (OPC) and Portland limestone cement (PLC) were examined in this study. Two types of specimens were employed: 25-mm cement paste cubes for destructive tests including mass loss and strength loss, and mortar bars of 25 x 25mm x 285 mm, as per ASTM C1012, for length change, due to sulphate exposure. The size of the cubes was chosen to represent the typical cover in concrete.

3.1.1 Materials

Lafarge OPC Type GU according to CSA (Canadian Standard Association) and Holcim PLC were used in making specimens. The chemical compositions of the two cements are presented in Table 3-1. The CO₂ content in as-received cement was determined by infrared-based CO₂ analyzer. It was 1.9% in OPC and 6.6% in PLC, indicating that both cements had contained a portion of limestone. Based on their molar ratio, OPC had 4.3% of powder limestone and PLC 15.0%. They were interground with clinker. The Blaine fineness was 390 m²/kg for OPC and 500 m²/kg for PLC. To improve the early age hydration strength, PLC was ground finer. Granite sand with a fineness modulus of 3.0 was used in the mortar specimens to avoid the inclusion of carbonates from the aggregates.

Table 3-1: Chemical composition of the cements

Cement type	Weight percent (%)							
	CaO	SiO ₂	Al ₂ O ₃	Fe ₂ O ₃	MgO	Na ₂ O	SO ₃	CO ₂
OPC	63.1	19.8	4.9	2.0	2.0	0.85	3.8	1.9
PLC	59.8	20.6	4.5	2.7	1.7	0.6	3.2	6.6

3.1.2 Mixing and casting procedures

A water-to-cement ratio of 0.36 was used in the making of the cement paste samples and mortar bars to represent typical precast concrete products such as sewage pipes, masonry blocks and hollow core slabs. The aggregates used in the mortar bars were 1 part cement to 2.75 parts of granite sand by mass

as specified in ASTM C 1012. Four batches for cubes and four batches for mortar bars were prepared. They are (1) hydrated OPC paste or mortar; (2) carbonated OPC paste or mortar; (3) hydrated PLC paste or mortar and (4) carbonated PLC paste or mortar. For hydrated references, initial curing in mould was 28 h for paste cubes and 22 h for mortar bars in sealed condition, followed by demoulding and 27 d subsequent hydration, again in sealed condition. To facilitate carbonation curing with cement paste or mortar of w/c of 0.36, open air initial curing is necessary to reduce free water and allow carbon dioxide diffusion. It was done by 24 h open air curing at relative humidity (RH) of 27% for cubes and 22 h at RH of 30% for mortar bars, followed by 4 h carbonation curing and 27 d subsequent hydration in sealed condition. The curing regime that was used is shown in Table 3-2 and the curing conditions are given in Table 3-3.

Table 3-2: Curing regimes

Batch ID	Initial curing	Carbonation curing	Subsequent curing in sealed bag
Cement Paste			
OPC	28h sealed	n/a	27d
COPC	24h open air	4h	27d
PLC	28h sealed	n/a	27d
CPLC	24h open air	4h	27d
Mortar			
OPCM	22h sealed	n/a	27d
COPCM	18h open air	4h	27d
PLCM	22h sealed	n/a	27d
CPLCM	18h open air	4h	27d

The sealed hydrated reference, OPC, PLC, OPCM and PLCM, were kept in a sealed condition without water loss, prior to being exposed to the sulphate solution. COPC, CPLC, COPCM and CPLCM were the carbonated samples that underwent air curing at the relative humidity and temperatures shown in Table 3-3, prior to being carbonated. As specified previously, samples to be carbonated were air dried. Through the production of numerous batches, it was found that 24 hour initial air curing was most suitable for cement paste cubes. In the case of mortar, 18 hours of initial air curing was necessary to get optimal carbon uptake. The 24 hour and 18 hour initial air curing also accommodate to overnight shift. OPC and PLC samples were prepared the exact same way. Therefore OPC and

PLC were comparable. In total, 40 cement paste cubes and 3 mortar bars were cast for each batch.

Table 3-3: Environmental conditions during mixing and open air curing

Batch ID	Temperature (°C)	Relative Humidity (%)
Cement Paste		
OPC	25	sealed
COPC	24	27
PLC	23.4	sealed
CPLC	24	27
Mortar		
OPCM	23.9	sealed
COPCM	23.9	30
PLCM	23.9	sealed
CPLCM	23.9	30

To compensate water loss during initial air curing, the carbonated specimens were water sprayed right after the 4 hour carbonation curing to restore their original water content and then sealed for a subsequent hydration of 27 days.

3.1.3 Carbon dioxide curing and uptake

As mentioned previously, specimens were carbonated following initial air curing. The early carbonation curing setup is illustrated in Figure 3-1.

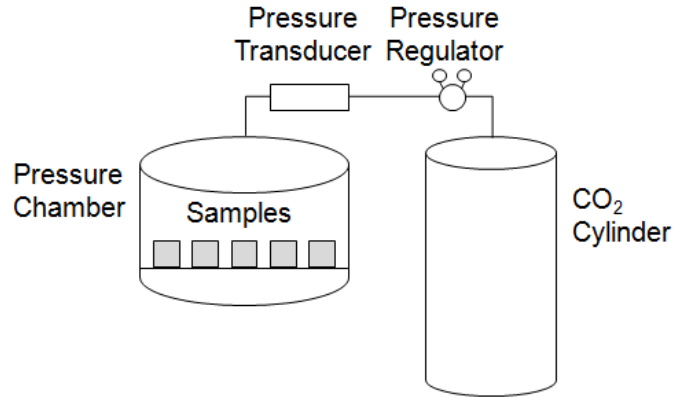


Figure 3-1: Carbonation setup

After initial open air curing, specimens were placed in a pressure chamber as shown in Figure 3-1. Carbon dioxide of 99.5% purity was injected and kept at a constant pressure of 0.15 MPa. The pressure was monitored and verified using a pressure regulator. Both mortar and paste specimens were carbonated for a period of four hours.

Two approaches were used to determine CO₂ uptake: the mass gain method and carbon analysis. The mass gain method compares the sample mass before and after carbonation. The mass difference, together with the water lost due to exothermic reactions, represents the carbon uptake. The lost water was collected by absorbent paper and added to final mass after carbonation. The equation for the mass gain method can be summarized as such:

$$CO_2 \text{ uptake } (\%) = \frac{Mass_{after \text{ carbonation}} + Mass_{water \text{ lost during carbonation}} - Mass_{before \text{ carbonation}}}{Mass_{cement}} \quad (3.1)$$

Percent CO₂ uptakes were calculated based on cement including limestone as part of binder mass. Carbon analysis was also used as an independent method to determine carbon uptake, and validate the mass gain equation. The analysis was performed using the ELTRA CS-800 Double Dual Range Carbon/Sulfur Determinator.

3.2 Sulphate exposure conditions

Following 28 days of curing in the regime described in Table 3-2, the samples were fully submerged in a 5% (w/w) magnesium sulphate (MgSO₄) solution. The fully submerged samples were kept at a temperature of approximately 5°C. Epsom salt (Magnesium Sulphate Heptahydrate acquired from Ore inc.) was used as the source of sulphate. The pH of the MgSO₄ solution was approximately 8.5. The sulphate solution was replaced every 3 months to avoid variations of pH. During the 3 month interval, the pH of the solution containing samples increased to approximately 10. The pH exposure from the sulphate solution was the same for all samples.

The submerged samples were kept at 5°C, as low temperatures have been found to promote thaumasite formation. The samples were therefore stored in a refrigerator, shown in Figure 3-2. The cement paste cubes and mortar bars were stored separately.



Figure 3-2: Low temperature sulphate attack test setup

A concentration of 5% was chosen as specified in ASTM C1012. Magnesium sulphate was chosen as it was suggested in the Durability Guide of ACI 201 Committee that groundwater containing $MgSO_4$ is more aggressive (Irassar 2009). Therefore, by submerging the samples in 5% $MgSO_4$ at $5^\circ C$, it was possible to get a good assessment of the long term behavior of the samples in harsh conditions. More importantly, it was possible to assess the resistance of the carbonated cements to low temperature sulphate attack, and compare its resistance to reference hydrated counterparts. All specimens were exposed to the exact same conditions in terms of temperature and solution, and are therefore comparable.

3.3 Testing

The purpose of the experiments conducted was to quantify the resistance of carbonated cements to thaumasite formation. The mortar bars were used to monitor the expansion that may be caused by TSA, as per ASTM C1012. The cement paste was used for all the other experiments that were performed. The use of cement paste in place of concrete or mortar was an attempt to avoid inclusion of aggregates and their influence on quantitative mineralogical analysis. As well, the prevalent reactions that come in play in this research, namely the carbonation and TSA reactions, occur directly on cement.

The experiments conducted on the paste and mortar bars are shown in Table 3-4. The resistance of cement paste cubes to thaumasite was monitored throughout the exposure period. The physical and mechanical resistance was verified by visual rating, mass loss and compressive strength. Crushed Samples were preserved in acetone to stop further hydration. The fractured samples from compressive strength tests were collected and ground to powder for phase analysis by XRD. TGA and Raman spectroscopy were conducted to further assess the mineralogy. Surface air permeability and pH of cement paste cubes were also determined.

Table 3-4: Tests performed on pastes and mortars

Sample type	Test	Time of Test
Cement Paste Cubes	Visual Inspection	After carbonation, prior to and at 1,2,4,6 and 10 months of MgSO ₄ exposure
	Mass Loss	After carbonation, prior to and at 1,2,4,6 and 10 months of MgSO ₄ exposure
	Compressive Strength	After carbonation, prior to and at 1,2,4,6 and 10 months of MgSO ₄ exposure
	X-Ray Diffraction (XRD)	After carbonation, prior to and at 1,2,4,6 and 10 months of MgSO ₄ exposure
	Thermogravimetric Analysis (TGA)	At 10 months of MgSO ₄ exposure
	Raman Spectroscopy	At 10 months of exposure to MgSO ₄
	Surface Air Permeability	Prior to MgSO ₄ exposure
	pH	Prior to MgSO ₄ exposure
Mortar Bars	Change in length (ASTM C1012)	At 1,2,3,4,8,13 and 15 weeks of MgSO ₄ exposure, followed by subsequent measurements at 4, 6 and 9 months

By assessing various deterioration indicators throughout the exposure period as shown in Table 3-4, it was possible to monitor the evolution of the deterioration over time. By comparing the deterioration of carbonated samples to hydrated reference samples, it was possible to assess the resistance of carbonated specimens.

Therefore, using data gathered from the experiments presented in Table 3-4, it was possible to quantify the resistance of carbonated samples over time using a variety of parameters. The procedure used to conduct each of these experiments is presented below.

3.3.1 Visual assessment

To help ascertain the degree of damage sustained by a specimen during the exposure interval, a visual assessment was conducted. Photographs were taken during these visual assessments. The inspections were carried out to evaluate the visible signs of surface deterioration such as spalling, cracking and softening in specimens exposed to sulfate attack and to link any such changes to variation in mineralogy and microstructure.

3.3.2 Compressive strength

Compressive strength measurements were obtained using the MTS Sintech machine shown in Figure 3-3.



Figure 3-3: MTS Sintech

The compression area of one inch square was used, which corresponds to the side of the cube, as shown in Figure 3-4. A minimum of three samples of each batch were tested to produce a representative average.



Figure 3-4: Compression strength tests

This mechanical test is a good indicator of damage to the cement paste that may be caused by the softening of the paste. In turn, the softening of the paste causes a decrease in compressive strength. Therefore, the resistance of the paste to thaumasite can be assessed using this indicator. Compressive strength results also provide useful information with regards to the effect of carbonation on the rate of hydration of specimens at early age.

3.3.3 Change in mass

The change in mass of the cement paste cubes was monitored using an electronic scale with a precision of 0.001g. The mass of the same four samples from each group was recorded throughout the exposure period. The mass was recorded when the samples reached a Saturated Surface Dry (SSD) condition, which corresponded to 10 minutes of open air drying at a RH of approximately 27% at ambient temperatures. The change in mass can provide an insight in the

deterioration of specimens due to spalling of the outer layer. In turn, the spalled material causes a decrease in mass. Using this parameter, the amount of spalled material can be monitored. This information provides insight into the resistance of samples.

3.3.4 Change in length

Change in length of the mortar bars was monitored with a precision of 0.001 mm using a length comparator. The procedure specified in ASTM C1012 was followed. The deviations from the ASTM procedure, highlighted in Table 3-5, were necessary to induce conditions favorable to the formation of thaumasite, and ensure that the mortar bars were comparable to the cubes.

Table 3-5: Deviations between current research and ASTM C 1012

	ASTM C 1012	Current Research
Curing	35°C for first day	24°C for first day
Time of immersion	20 MPa (~1 day)	28 days
Solution	Sodium sulphate	Magnesium sulphate
Aggregate type	Silica sand (C109)	Granite sand
W/c	0.485	0.36
Change of solution	With measurements	Every 3 months
Storage temperature	23°C	5°C

The setup for length measurements is shown in Figure 3-5.



Figure 3-5: Change in length of mortar bar measurements

Expansion is an indicator of traditional sulphate attack. The expansion is caused by the formation ettringite rods in hardened concrete. It was essential to monitor change in length to determine whether ettringite was also present in deteriorated samples. If so, the change in length gives insight into the resistance of carbonated samples to ettringite. However, the replacement of C-S-H by thaumasite reportedly results in softening of the cement paste matrix into a

white, mushy non-cohesive mass (Crammond 2003). Therefore, monitoring expansion does not give insight into the formation of thaumasite.

3.3.5 X-Ray Diffraction (XRD)

Phase analysis of the cement paste samples was conducted using XRD (Phillips PW1710, Cu K α radiation, scan interval 5-45° 2 θ , 0.02° and 0.5 s per step). Powders samples were taken from the outer 2mm surface. This region was studied as it was fully carbonated. As well, the sulphate attack will start from the exterior of the sample, as TSA is an external form of sulphate attack. Furthermore, by studying the exterior surface, it is possible to know if thaumasite is formed, but also after how many months of sulphate exposure. Therefore, this region was found to be the most indicative of the resistance of carbonated paste to TSA as the deterioration occurred.

The main purpose for XRD was to track mineralogy changes that may be caused by TSA, and detect sulphate attack compounds as they form throughout the deterioration. These compounds include thaumasite, gypsum and ettringite. It was indispensable to use XRD as it is reportedly one of the most efficient methods to distinguish ettringite and thaumasite. Phase analysis by XRD was also conducted prior to exposure to the sulphate solution. The objective was to distinguish the mineralogy between carbonated and hydrated pastes.

3.3.6 Thermogravimetric analysis and differential thermal analysis

Thermogravimetric analysis (TGA) and Differential Thermal Analysis (DTA) were performed using approximately 200 mg of the same powder sample used for XRD. For TGA, the Differential Thermogravimetric Analysis (DTG) is

presented. A thermal analyzer (NETZSCH, TG 449 F3 Jupiter) with a resolution of 0.01 mg was employed to run TGA and obtain the mass loss of the specimens in the range of 25°C to 950°C at a heating rate of 10°C/min. DTA was used in an attempt to help identify thaumasite. TGA/DTA were also used to help distinguish between the carbonates already present in OPC and PLC cement from limestone addition and the carbonates produced during carbonation.

3.3.7 Raman spectroscopy

The molecular composition of deteriorated cement paste specimens was also assessed using Raman spectroscopy. A Bruker Optics Senterra System equipped with a 532 nm laser at 20 mW amplitude was used to gather Raman spectra. Similarly to TGA, the powder was gathered from 2-mm surface of the samples that had been fully submerged in a magnesium sulphate solution at 4°C for 10 months. In the case of PLC samples, both spalled material and core material were tested to study the depth of the sulphate attack within the specimen.

3.3.8 Surface air permeability

In order to compare the surface air permeability of the four groups of cement paste cubes, a poroscope (James Instrument Inc, Model P-6050) was used. The poroscope included a steel chamber to be clamped to the surface of the samples. The chamber is sealed and subsequently subject to a vacuum. The chamber is then connected to the instrumentation. In turn, the instrumentation is connected to a hand vacuum pump. The test apparatus is shown in Figure 3-6.

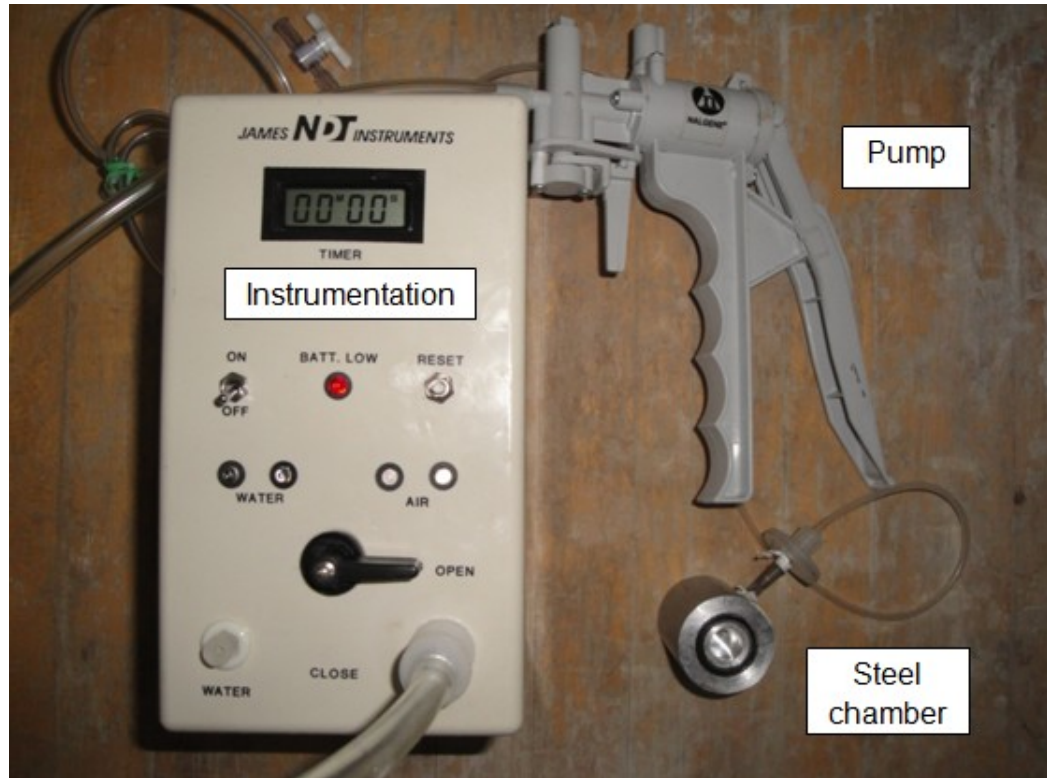


Figure 3-6: Surface air permeability test apparatus

The pump provides a negative pressure of -55 kPa in the chamber. Meanwhile, the instrumentation measures the time required for the negative pressure in the chamber to climb to -50 KPa. The parameter considered to be representative of the surface air permeability of the cement paste cubes was the time it took for the vacuum pressure to increase by 5 kPa. The steel chamber provided by the manufacturer was however too wide for the cubes. Therefore, a narrower steel chamber was built with the exact same volume as the steel chamber provided with the instrument. The setup is shown in Figure 3-7 below.



Figure 3-7: Surface air permeability test setup

Surface air permeability was considered an important factor due to the nature of TSA. Being an external form of sulphate attack, the permeability of a sample has a great influence on the associated damage, as the sulphate must first enter the sample before the reaction proceeds.

3.3.9: pH measurements

The pH measurements were taken using a pH meter (Extech PH110) equipped with a flat sensor head of 9mm in diameter. An ion extraction method was used for the pH measurements of cement paste specimens. An absorbent paper was placed on the paste, and 100 μ l was dropped on the absorbent paper.

After 15 minutes, the pH of the solution extracted by the paper was measured. The pH measurements of three specimens in each batch were taken and the values were averaged.

Chapter 4: Results and Discussions

The experimental results are presented in this chapter. The first section of Chapter 4 focuses on the early age carbonation curing and carbon dioxide uptake of the cement pastes and mortar bars. The process was developed to simulate large scale concrete production. The second section discusses the effect of carbonation on the Thaumassite form of Sulphate Attack (TSA). The results allowed for a comparison of the resistance to TSA in carbonated and hydrated specimens. The third section of this chapter studies the mineralogy of hydrated and carbonated OPC and PLC by XRD, TGA/DTG, DTA and Raman spectroscopy. Therefore, this section provides insight into the chemical changes throughout the exposure period. In the last section, further investigations are presented in an attempt to understand the mechanism of the resistance of carbonated and hydrated cement pastes to thaumasite formation.

4.1 Early carbonation curing of cement pastes and mortar bars

Carbonation curing of cement paste cubes and mortar bars was carried out. The degree of carbonation was assessed by CO₂ uptake, which was obtained using two methods, mass gain method and infrared based carbon analyzer method. Phase analysis of pastes was performed using XRD to assess the effect of carbonation on the mineralogical change. Compressive strength measurements were also conducted in order to monitor the rate of hydration.

4.1.1 Carbonation curing and CO₂ uptake

Carbonation curing is strongly dependent on water content in cement paste. While too much water will impede gas diffusion, too little will hinder the process of dissolution and precipitation. To facilitate carbonation of a cement paste with w/c of 0.36, preconditioning by open air curing was necessary. Table 4-1 shows the water content change during the carbonation curing.

Table 4-1: Water content change during carbonation curing

Water content with respect to mixing water (%)					
Batch ID	After mixing	After air curing	After carbonation	After water spray	Remaining water
<i>Cement paste cubes</i>					
OPC	100	n/a	n/a	n/a	100
COPC	100	68	66	100	100
PLC	100	n/a	n/a	n/a	100
CPLC	100	73	71	100	100
<i>Mortar bars</i>					
OPCM	100	n/a	n/a	n/a	100
COPCM	100	76	73	100	100
PLCM	100	n/a	n/a	n/a	100
CPLCM	100	76	73	100	100

After 18-24 hours open air curing at ambient temperature and at 27-30% relative humidity (RH), approximately 25-35% of free water was removed. This step was necessary to create space for carbonate precipitation. The carbonation curing that followed did not evaporate additional free water. The lost water during preconditioning was compensated by water spray to surface saturation. The final carbonated specimens had comparable water content to hydration references, which were cured in sealed condition without water loss.

The CO₂ uptakes by pastes and mortars through carbonation measured by mass gain and carbon analyzer methods are presented in Table 4-2.

Table 4-2: CO₂ uptake of cement paste and mortar

Batch ID	CO ₂ Content (%)	CO ₂ Uptake (%)	
		Carbon analyzer	Mass gain
As Received Cement			
OPC	1.62	n/a	n/a
PLC	6.97	n/a	n/a
Cement Paste			
OPC	2.22	n/a	n/a
COPC	Surface: 6.87 Core: 2.81 Average: 4.89	Surface: 5.25 Core: 1.19 Average: 3.19	4.23±0.26
PLC	6.70	n/a	n/a
CPLC	Surface: 11.43 Core: 6.92 Average: 9.18	Surface: 4.46 Core: 0 Average: 2.23	4.95±0.73
Mortar			
OPCM	n/a	n/a	n/a
COPCM	n/a	n/a	5.40±0.55
PLCM	n/a	n/a	n/a
CPLCM	n/a	n/a	6.2±0.71

CO₂ contents measured by infrared based carbon analyzer in as-received cements represented the initially existing limestone additive. The CO₂ content in both hydrated and carbonated cement pastes were determined in terms of dry cement mass used in specimens. The difference in CO₂ contents between the carbonated and the as-received cements represented the CO₂ uptake by

carbonation curing reaction. As expected, the initial CO₂ content in hydrated PLC was higher than that of hydrated OPC, due to the carbonates from the limestone filler. The equivalent CaCO₃ was 5.0% in hydrated OPC pastes and 15.2% in hydrated PLC pastes.

The carbon analysis results also showed that carbonation progressed from the outside to the inside of the specimen, as more carbonation reaction happened at the surface. In the case of carbonated PLC, there was no carbonation at the core. The difference in carbon content was expected as the CO₂ was directly in contact with the outer surface. On the other hand, for the core to receive carbonation, the gas had to travel through the surface in the specimen. The mass gain results were in the same order of magnitude as the carbon analysis results, although slightly higher than the average of carbon analysis. The CO₂ uptake results were similar in both OPC and PLC. However, due to the initial limestone filler present in PLC, the carbon content in carbonated PLC specimens was much higher in PLC than in OPC. The CaCO₃ content for the four cements is shown in Table 4-3.

Table 4-3: Equivalent CaCO₃ content of cement pastes

Batch ID	CaCO ₃ content (%)
OPC	5.0
COPC	15.6
PLC	15.2
CPLC	25.9

CPLC had calcium carbonates both added in cement as limestone filler by the manufacturer, and produced from the carbonation reaction. It is important

to note that as received OPC also contained carbonates. Indeed, many standards such as CSA and ASTM allow cement manufacturers to include up to 5% limestone filler in OPC. The mortar bars had shown a similar carbon uptake. Like the cement paste cubes, carbonated PLC mortar bars had a higher uptake than carbonated OPC specimens. The higher carbonation in PLC cement was attributed to finer particle size and higher water-to-clinker ratio in paste.

4.1.2 Phase analysis by x-ray diffraction

Figure 4-1 shows the XRD patterns of paste specimens following carbonation and subsequent hydration. The peaks corresponding to Calcium Hydroxide (CH) were slightly consumed in carbonated specimens. The Calcium Carbonate (CC) peaks were amplified in carbonated specimens. Hydrated PLC had stronger calcium carbonate peaks than hydrated OPC due to the presence of limestone powder. The carbonated OPC showed amplified calcium carbonates similar to hydrated PLC because their CaCO_3 contents were in the same range, the former being 15.6% and the latter 15.2%. Carbonated PLC had shown much stronger CaCO_3 peaks corresponding to CaCO_3 contents of 25.9%, due to the limestone addition and carbonation curing. This observation confirmed the formation of calcium carbonates through the carbonation curing reaction, and the consumption of CH.

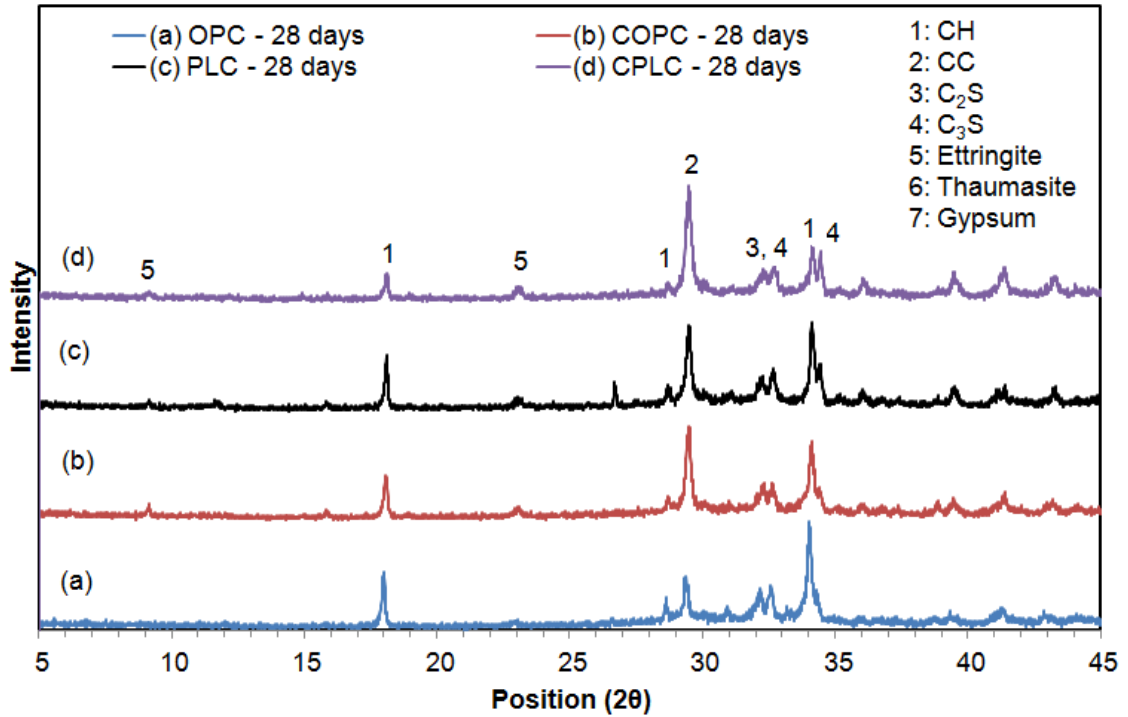


Figure 4-1: XRD patterns of pastes after 28 days of curing

4.1.3 Compressive strength

The compressive strength of cement pastes is a good indicator of hydration and carbonation curing. Figure 4-2 shows the compressive strength of cement paste cubes after 28 hours and 28 days of curing. For hydrated references, the cubes were sealed in plastic containers and tested at 28 hours and 28 days. There was no water loss during curing. For carbonated pastes, the cubes went through a process that involved 24-hour open air curing, 4-hour carbonation curing and water compensation to surface saturation. Three specimens per batch were then tested for average right after carbonation to determine the 28-hour strength and more were sealed for continued hydration to 28 days.

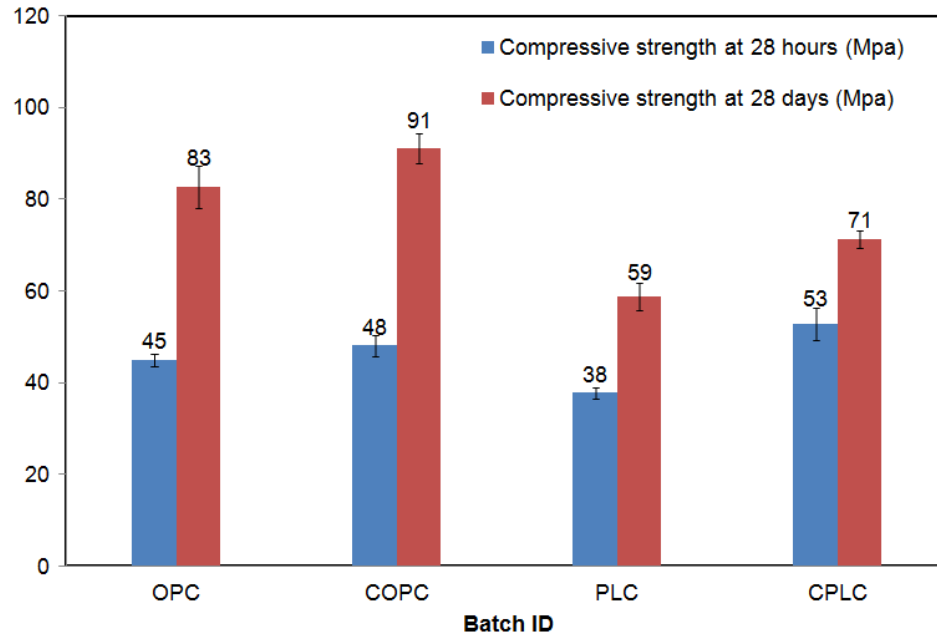


Figure 4-2: Compressive strength of cement pastes after 28 hours and 28 days of curing

While the compressive strength of carbonated OPC specimens was comparable to hydrated specimens right after carbonation, despite losing a significant amount of water during the curing period, the carbonated PLC actually had a higher strength right after carbonation than hydrated PLC. This increase in strength in carbonated PLC was attributed to the higher carbon uptake found in CPLC. Hydrated PLC had exhibited lower strength than the hydrated OPC even though PLC had a finer particle size. It was the clinker content that was more dominant in strength gain. At 28 days, carbonated and hydrated specimens had very similar strengths. Therefore, it was apparent that the carbonated specimens were able to reach similar strength than hydrated specimens, as long as the initial water content was restored by water compensation following air curing and carbonation curing. At 28 days, OPC specimens were found to have a much

higher compressive strength than PLC specimens. The difference in strength was attributed to a higher amount of clinker in OPC, allowing for the formation of more hydration products.

4.2 Thumasite formation in hydrated and carbonated OPC and PLC

After 28-day curing, four batches of specimens: hydrated OPC, carbonated OPC, hydrated PLC and carbonated PLC, were immersed in a 5% MgSO_4 solution at 5°C to test for thaumaiste form of sulphate attack (TSA). In order to assess thaumasite-formation in different cements and mortars, multiple indicators of deterioration were used throughout the exposure period. They included visual assessment, mass loss, compressive strength change of cement paste cubes, as well as length change of mortar bars. These indicators were used to compare the deterioration of carbonated and hydrated specimens, and assess the resistance of these specimens to TSA.

4.2.1 Visual inspection

Firstly, a visual inspection of the cement paste specimens was performed regularly throughout the exposure period. Photographs were taken during the inspection. Figure 4-3 shows the specimens after 6 months of submersion in a 5% MgSO_4 solution, at 5°C. Visually, OPC specimens did not appear to have any major deterioration after 6 months of exposure. Carbonated OPC specimens also did not show any major sign of deterioration. Hydrated PLC specimens seemed to have suffered the most damage. Damage in PLC specimens started with damage at the corners, followed by cracking in the direction of the edges of

the cubes. The damage was clearly due to the loss of cohesion in the CSH binding phase leading to a mushroom-type spalling. The damage in PLC specimens was attributed to the presence of the higher percentage of limestone filler. Similar damage was also reported by other researchers (Kakali et al. 2003, Tsvilis et al. 2007, Torres et al. 2004). However, despite the presence of the same amount of limestone filler and additional carbonates from carbonation, carbonated PLC specimens did not show any spalling damage after an exposure of 6 months. Instead, carbonated PLC specimens maintained a perfect surface around all sides of the cube, including the corners. The carbonation process changed the way the cement paste was reacting to the sulphate solution. When taking photographs, it was not possible to clean out the white powder on the outer surface of hydrated specimens, whereas the similar white powder layer on outer face of carbonated specimens was easily removed. This phenomenon is also noticeable in Figure 4-3, where it is nearly impossible to see the numbering of hydrated specimens, as opposed to the clean surface of carbonated specimens.

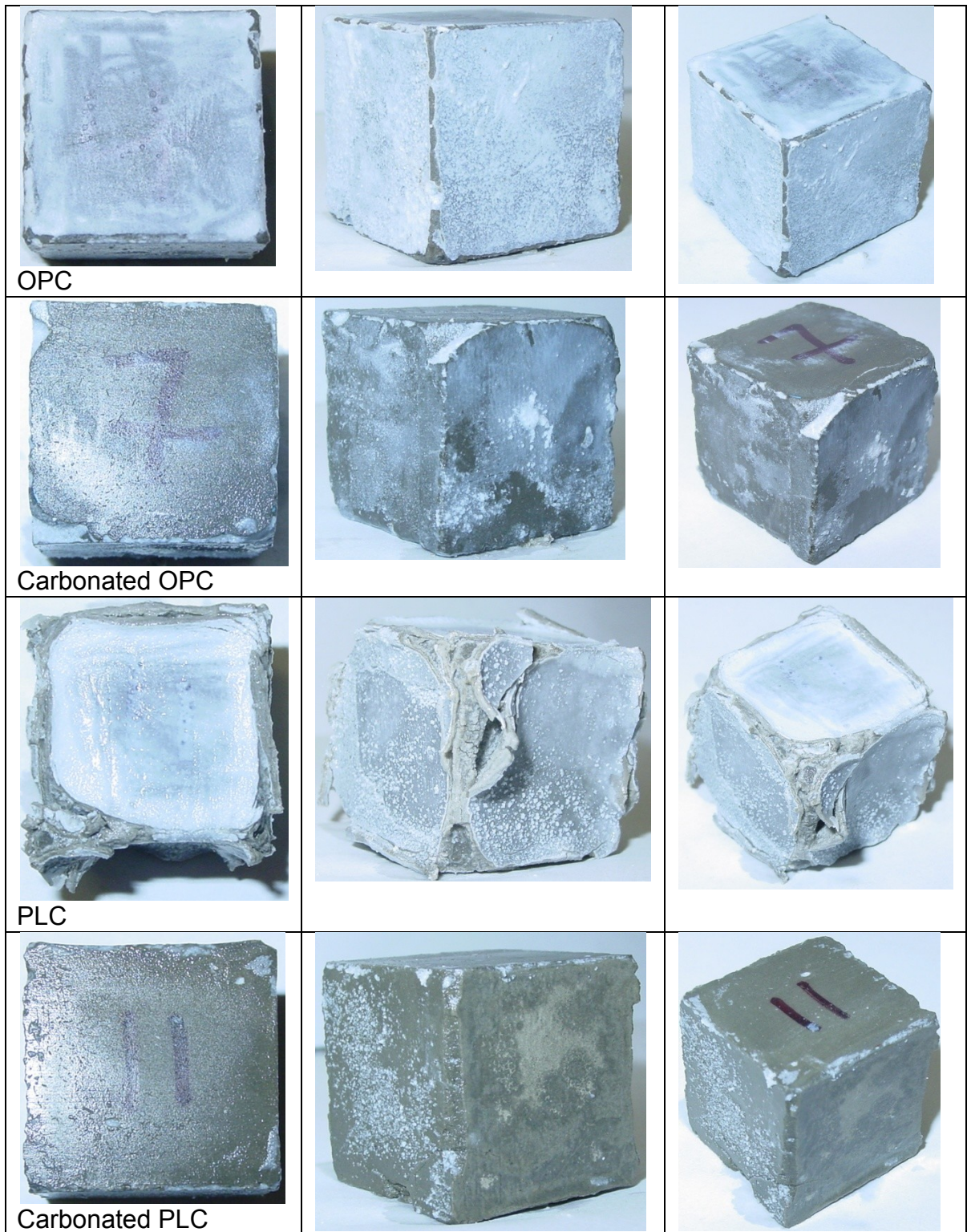


Figure 4-3: Cement paste cubes after submerged in a 5% MgSO₄ solution for 6 months at 5°C

Figure 4-4 displays the specimens after 10 months of submersion to the magnesium sulphate solution, at 5°C. At this stage of exposure, there was no visible damage in hydrated OPC specimens. Carbonated OPC specimens still did not show any apparent sign of deterioration. PLC specimens underwent extensive cracking, spalling and expansion. The outside surface was almost completely spalled off in all specimens. When comparing this image to that of 6 months, it is clear that the reaction in PLC had progressed considerably during this period. Therefore, it was concluded that the deterioration increased in hydrated PLC with an increased exposure time. Nevertheless, carbonated PLC specimens still did not show any sign of deterioration. Also, once more, when taking photographs, it was not possible to clean the white powder on outer surface of the hydrated OPC specimens, whereas the outer face of carbonated specimens was easily cleaned and the white layer removed. Therefore, visually, it can be concluded that the resistance of carbonated PLC specimens is improved. Both hydrated and carbonated OPC had shown excellent resistance to TSA. While hydrated OPC contained 5.0% ground limestone and was not vulnerable to TSA, the carbonated OPC had a 15.6% CaCO₃ content, which was of close value to hydrated PLC. Nevertheless, carbonated PLC was much more resistant to TSA than hydrated PLC, despite having a CaCO₃ content of 25.9%.

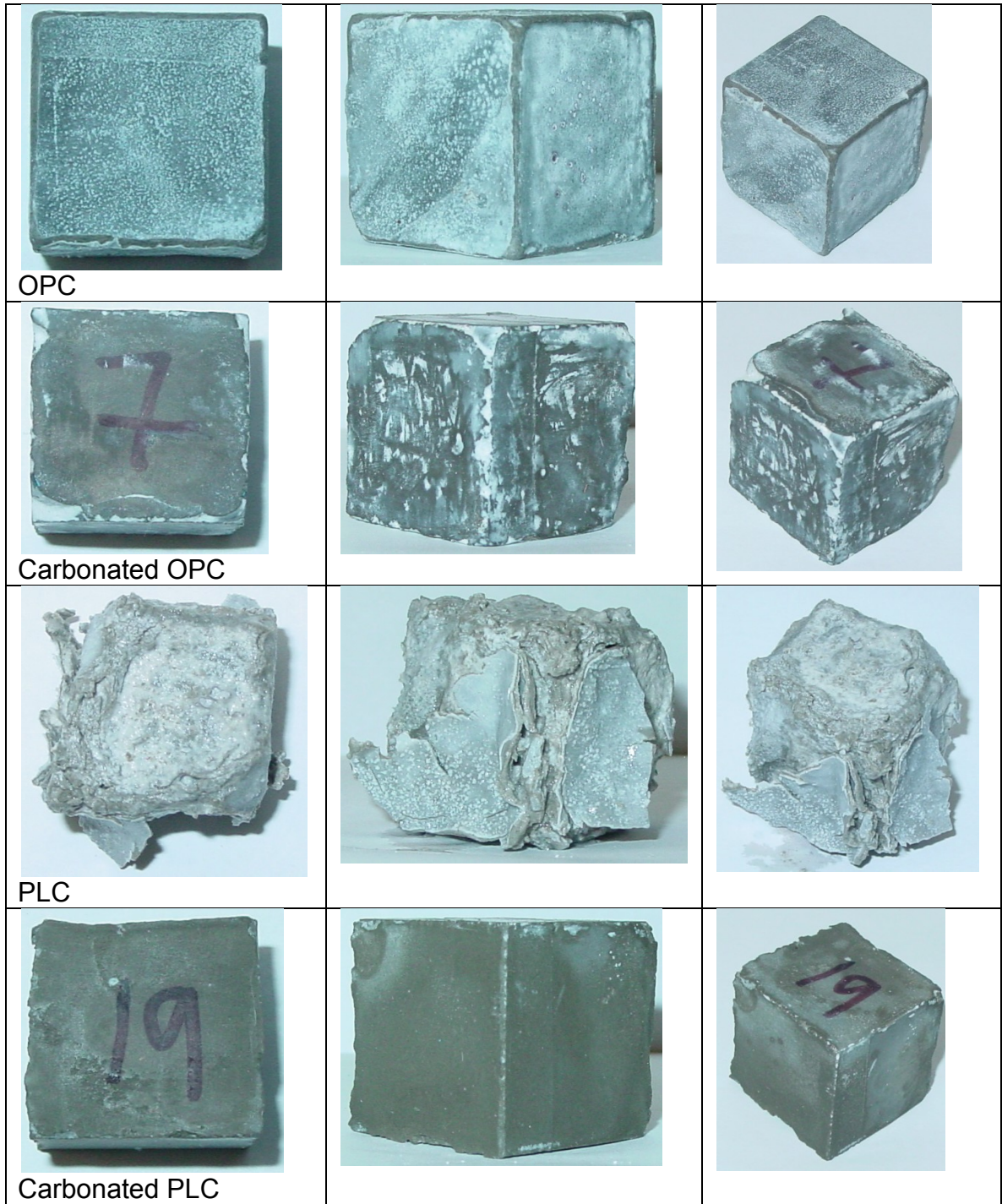


Figure 4-4: Cement paste cubes after submerged in a 5% MgSO₄ solution for 10 months at 5°C

4.2.2 Mass loss

Another indicator of thaumasite-induced damage is mass loss in specimens, which can be caused due to spalling of the outer layer of specimens. The spalling of specimens is caused by a loss of cohesion due to the decalcification of the CSH. In turn, the decalcification of the CSH causes the loss in cohesion of concrete. Therefore, to help assess the thaumasite-induced damage, the mass of the cement paste specimens was monitored throughout the exposure period. The average mass of four specimens throughout the exposure period is shown in Figure 4-5.

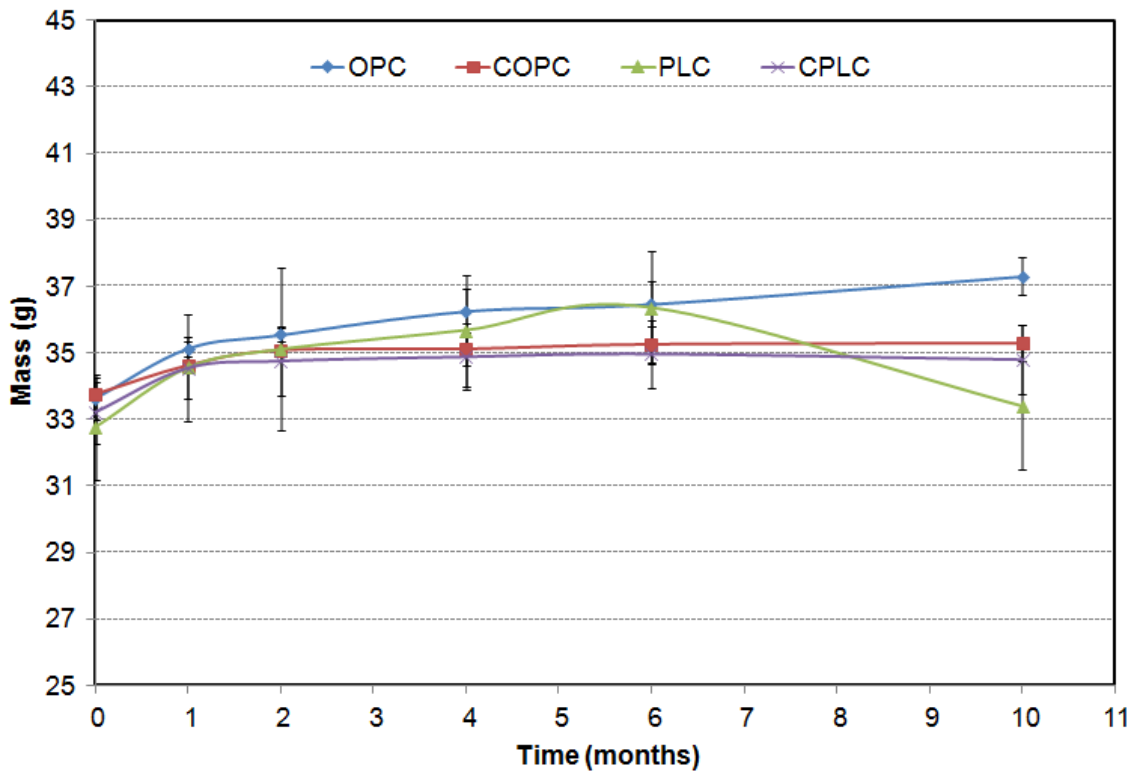


Figure 4-5: Mass change of cement paste cubes versus time
Mass change of cement paste cubes versus time

The mass of the hydrated OPC specimens increased for the entire 10 months of exposure, as shown in Figure 4-5. The increase in mass was attributed to the specimens absorbing the sulphate solution. As well, hydrated OPC specimens were not deteriorated to the point of spalling up to 10 months of exposure. There was no mass loss in hydrated OPC.

Hydrated PLC specimens had also seen a mass increases in the first 6 months of exposure, owing to the spalling and absorption of the sulphate solution. The mass of PLC specimens at 6 months was still above the mass prior to exposure, despite some material being slightly lost by spalling, as shown previously.

Both carbonated OPC and PLC specimens had seen an increase in mass during the first month of exposure. During the following 9 months of exposure, the specimen mass difference was negligible. From this result, it was concluded that hydrated specimens were more absorptive, which could indicate that an open structure was generated. The resilience of carbonated specimens to absorb the sulphate solution could be explained by the densification of the pore structure on the specimen surface during carbonation. This phenomenon can also be seen in Figure 4-6.

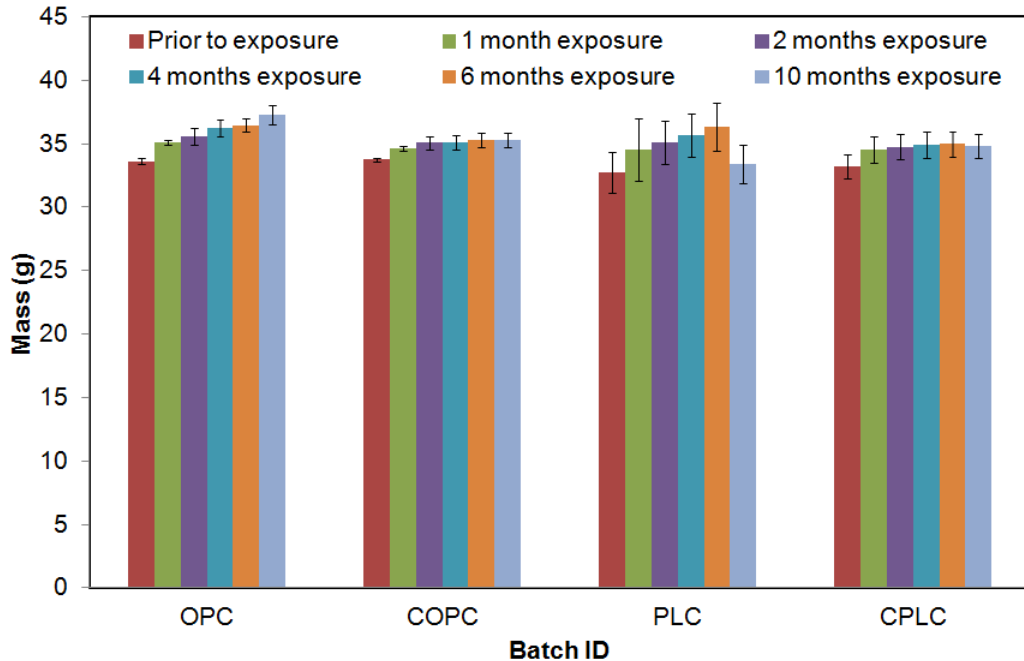


Figure 4-6: Mass change of cement paste cubes

As mentioned previously, the only mass loss happened in PLC specimens, and occurred between 6 and 10 months of exposure to the sulphate solution. However, mass was lost from these specimens at 6 months of exposure, but was offset by the mass gain due to the absorption of sulphates in specimens. Therefore, mass loss has not proven to be a valid indicator of sulphate attack induced damage at early age of the deterioration. This indicator should become more representative at later stages of the deterioration, where mass loss is expected to be more significant, and will offset the absorbed solution. Results showed that carbonation reduced the absorption due to the smaller increase in mass. Therefore, less damage would be expected with less ingress of sulphates in the specimens. The comparison in mass loss between PLC and CPLC did indicate that carbonated specimens were more resistant to thaumasite formation, which was in accordance with visual inspection results.

4.2.3 Compressive strength

Thaumasite induced damage can also cause a decrease in the compressive strength of cement in later stages of the deterioration. Compressive strength is not the best indicator of cracks caused in conventional sulphate attack due to the ettringite formation, as the mechanical test tends to close cracks. However, with thaumasite induced damage, the deterioration causes loss of cohesion of concrete. As the deterioration progresses, the concrete can even turn to mush. Therefore, the compressive strength of the cement paste cubes was also monitored to study the resistance of carbonated specimens subject to TSA. Compressive strengths of the cement paste specimens are shown in Figure 4-7.

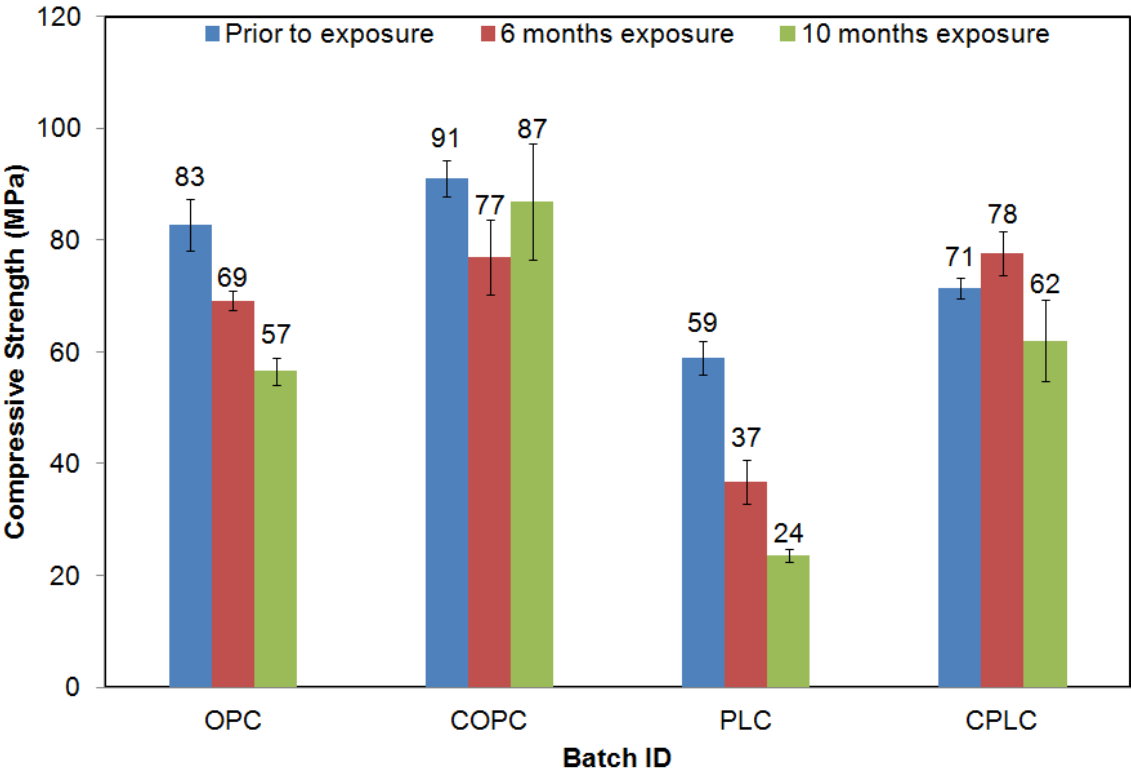


Figure 4-7: Compressive Strength of Cement Paste Specimens

The hydrated OPC specimens had seen a strength reduction of 17% at 6 months and 31% at 10 months, although there was no apparent mass loss due to TSA. This drop in strength could be explained by the formation of sulphate attack compounds such as ettringite and gypsum. The strength reduction in carbonated OPC was much less. If the standard deviation was considered, the change of strength was negligible, indicating that the carbonated OPC was more resistant to TSA.

As expected from the visual and mass loss results, hydrated PLC specimens experienced a significant decrease in compressive strength, which was very noticeable after 6 months of exposure, with a strength reduction of 32%. The drop in strength was more pronounced after 10 months of exposure, corresponding to a strength reduction of nearly 60%. The specimens had lost almost two thirds of their compressive strength owing to the significant loss of cohesion caused by TSA.

The carbonated PLC had seen a strength reduction of 13% at 10 months. Carbonated PLC specimens did appear however to have an increase in strength up to 6 months of exposure, which was attributed to continued hydration.

Based on compressive strength results, it was apparent that carbonation had an important effect on the resistance of paste subject to TSA. Similarly to the visual and mass loss results, the difference was especially noticeable when comparing hydrated and carbonated PLC specimens. It can be concluded that

carbonation improved compressive strength of otherwise identical specimens, when exposed to TSA.

4.2.4 Change in length

Another common physical parameter used to interpret the resistance of cement to sulphate attack is expansion. As discussed in Chapter 2, this test method is mainly relevant when testing for conventional sulphate attack. In this type of sulphate attack, the main deterioration is caused by the formation of ettringite rods in hardened concrete. In turn, ettringite rods cause expansion of the concrete. Inherently, thaumasite does not cause expansion, but rather loss of cohesion. Therefore, the ASTM C1012 standard test was modified to examine if ettringite was also being formed, causing expansion, in a 5% MgSO_4 solution at 5°C. As well, this test was useful to investigate if the main damage induced by thaumasite is due to expansion. Therefore, the ASTM C1012 standard was modified to assess the expansion of both hydrated and carbonated mortar bars at 5°C. The expansion of the hydrated and carbonated mortar bars, over the exposure period, is presented in Figure 4-8.

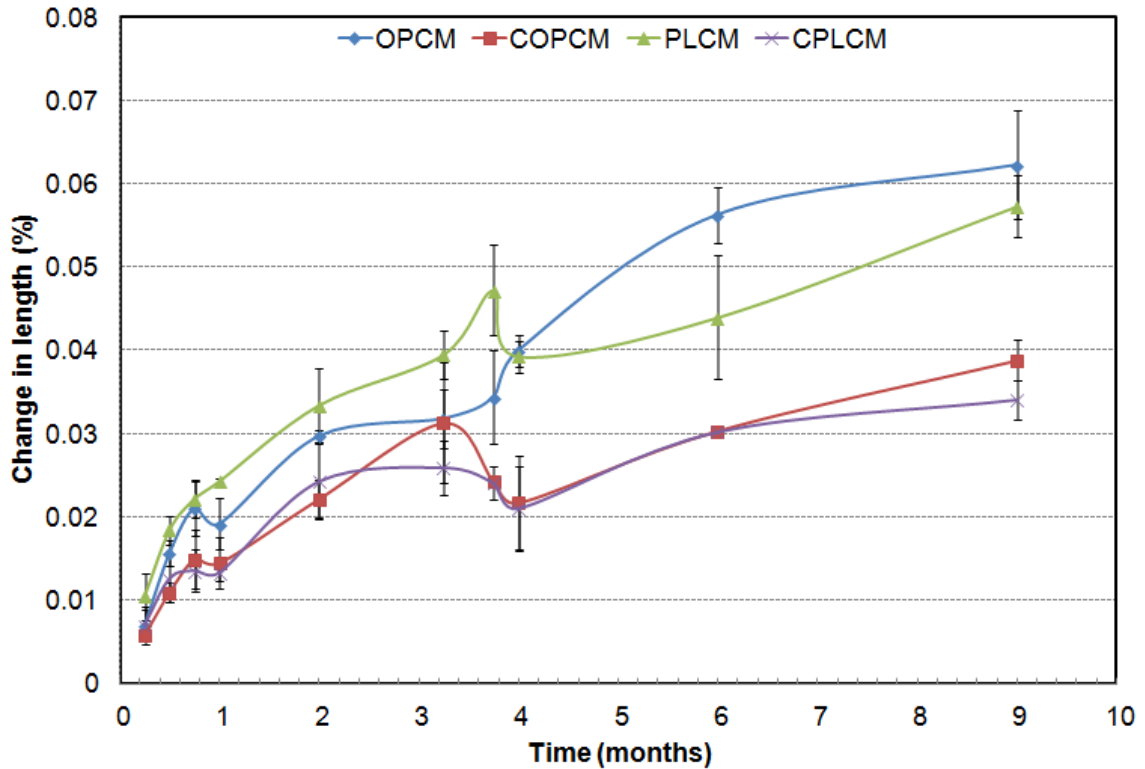


Figure 4-8: Expansion of mortar bars

Up to 4 months, the largest expansion was recorded for hydrated PLC specimens. Subsequently, hydrated OPC specimens expanded more for the remaining of the exposure period. The fact that both hydrated and carbonated cement pastes experienced expansion in a range of 0.03 to 0.06% was indicative that ettringite could be formed in cement pastes exposed to a 5% MgSO_4 solution at 5°C.

The limit for the ASTM C 1012 is 0.05 percent expansion after 6 months of exposure for this concentration of solution. Therefore, based on this limit, hydrated OPC and PLC were marginal while carbonated OPC and PLC were acceptable. However, it should be noted that some of the conditions specified in ASTM C1012 were modified, as mentioned previously. It was seen that

expansion was not the best indicator for TSA-induced damage since the hydrated PLC mortar bars also experienced significant cracking, spalling and mass loss, which did not translate to length change. It is demonstrated by Figure 4-9 in which hydrated PLC mortar bars were strongly deteriorated.



Figure 4-9: Mortar bars following 10 months of exposure to $MgSO_4$ at $5^\circ C$

However, PLC specimens showed less expansion than hydrated OPC specimens. Based solely on expansion, PLC specimens could be deemed acceptable as per the expansion limit presented above. Interestingly, the difference between specimens and their carbonated counterpart was very similar with OPC and PLC. Based on the results presented, it was seen that expansion was not a valid TSA indicator. This test has however shown that carbonation

decreased the expansion caused by sulphate attack, perhaps diminishing the occurrence of ettringite. Carbonated mortar does show improved resistance to ettringite based-expansion.

In conclusion, it was clear that the resistance to TSA loss of cohesion and ettringite form expansion was considerably improved in carbonated OPC and PLC in comparison with hydration counterparts. The improved durability properties were noticeable visually, as well as in terms of mass loss, compressive strength and expansion.

4.3 Effect of thaumasite form of sulphate attack on mineralogy of cement paste

The previous section was focused on damage that was caused by TSA. In this section, mineralogy analysis was performed to track and monitor sulphate attack minerals that may be formed during exposure to the sulphate solution. These sulphate attack products include thaumasite, gypsum and ettringite. XRD, TGA/DTG, DTA and Raman spectroscopy were used to characterise the mineralogy of specimens.

4.3.1 X-ray diffraction

The main tool used for mineralogy analysis was X-Ray Diffraction (XRD). This method is efficient to detect thaumasite and differentiate it from ettringite. The XRD patterns of ettringite and thaumasite are shown in Figure 4-10 (hartshorn et al., 1999). Thaumasite can be identified based on peaks at around 16, 23.5 and 28° 2 θ , which are not present in the ettringite pattern. The presence

of ettringite can be confirmed by its characteristic peaks at around 15.8, 18.9, 22.9, 25.5° 2θ (Kakali et al. 2003).

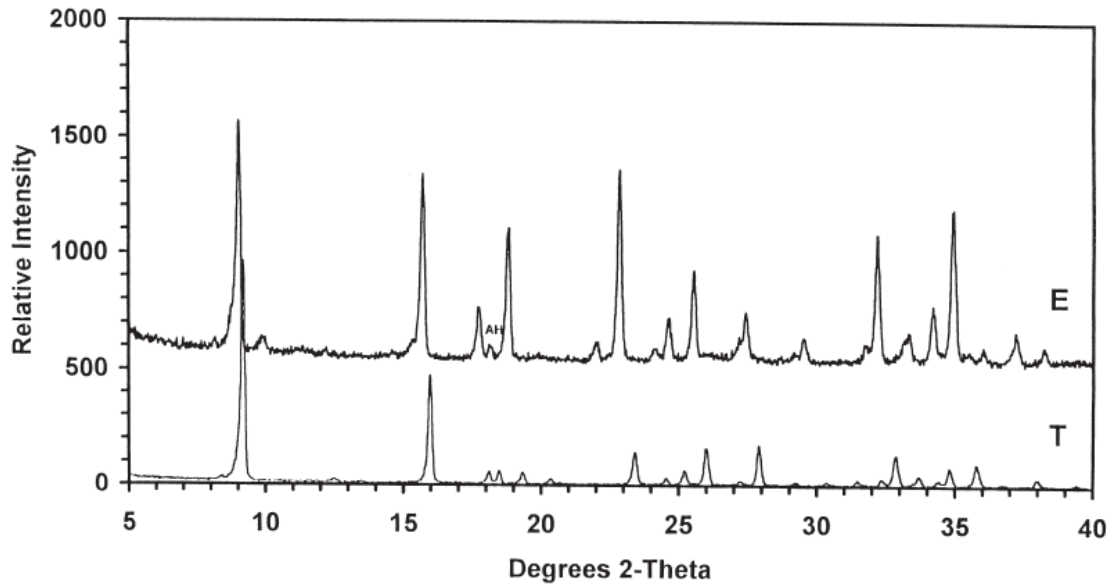


Figure 4-10: XRD patterns of ettringite (E) and thaumasite (T) (hartshorn et al., 1999)

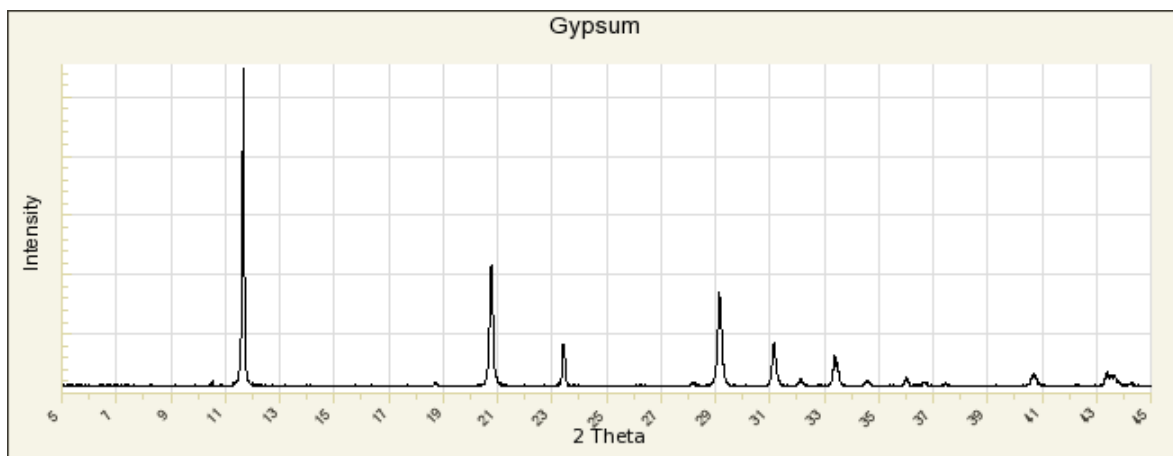


Figure 4-11: XRD pattern of Gypsum

The XRD pattern of gypsum is shown in Figure 4-11(Downs, 2006).

Every batch of cement paste cubes were tested for XRD throughout the exposure period. Figure 4-12 shows the XRD patterns for OPC specimens from 0 to 10 months of exposure to the sulphate solution. The 0 month measurement corresponds to the XRD pattern observed prior to submerging the specimens in the sulphate solution.

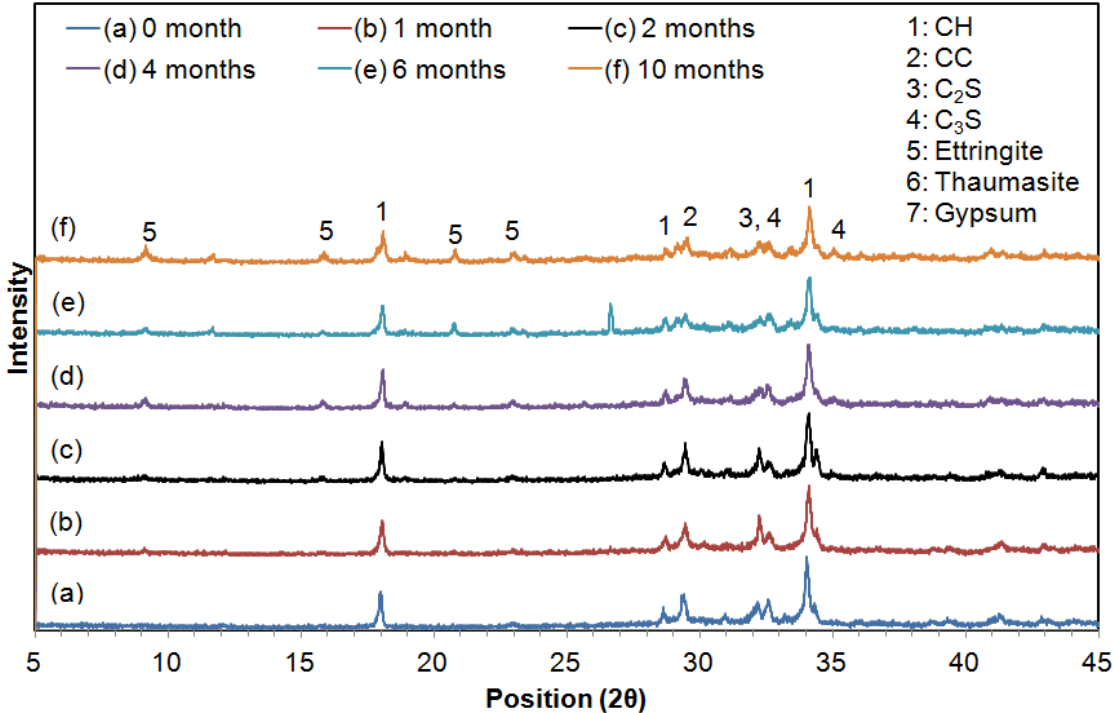


Figure 4-12: XRD pattern of hydrated OPC specimens

The patterns were relatively similar from 0 to 6 months of exposure. At 10 months, ettringite was detected in small amounts for the first time. There was no thaumasite present up to 10 months of exposure. The presence of ettringite confirmed the expansion measurements presented in Figure 4-8. The lack of thaumasite was attributed to the small amount of calcium carbonates in hydrated OPC (5.0%), although they were visible on the XRD pattern. It is also possible that thaumasite may form at later stages of the deterioration.

Figure 4-13 displays XRD patterns for carbonated OPC specimens throughout the exposure, from 0 to 10 months.

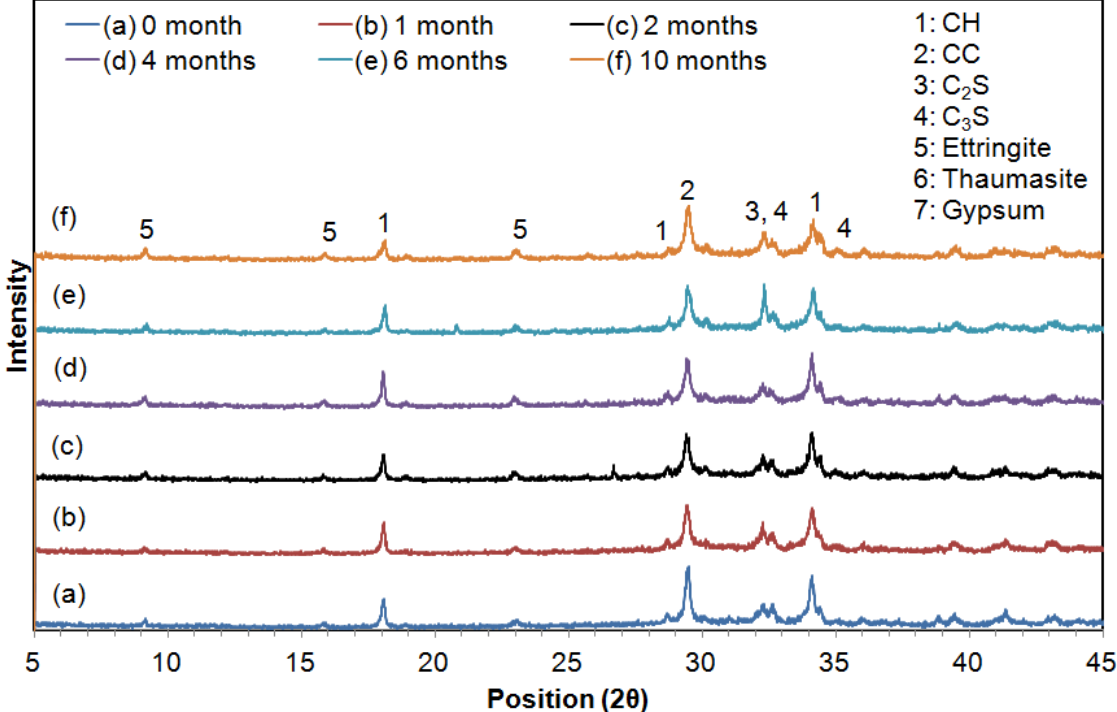


Figure 4-13: XRD patterns of carbonated OPC specimens

A small peak corresponding to ettringite, at around 9° 2θ, was found in carbonated specimens throughout the exposure. However, the peak was present before exposing the specimens to the sulphate solution and remained afterwards. Other significant ettringite or thaumasite peaks were not present. Therefore, it was concluded that no thaumasite or ettringite had formed from the sulphate solution up to an exposure time of 10 months.

Figure 4-14 shows the XRD patterns of PLC specimens throughout the exposure period. It is important to note that the outer layer of 3-mm was taken for

the analysis in all batches. Therefore, at 6 and 10 months, when specimens had spalled, the lost material was collected and tested for the XRD results.

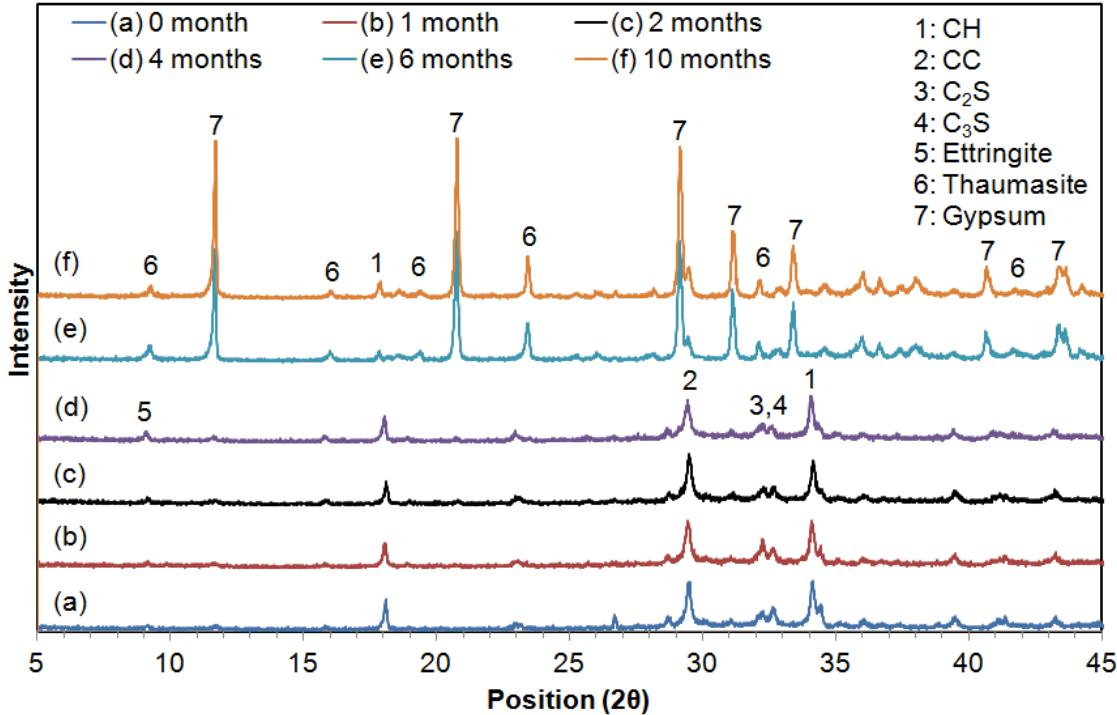


Figure 4-14: XRD patterns of hydrated PLC specimens

In order to assess the mineralogy of the core of deteriorated PLC specimens, phase analysis was also performed on the core of the specimen at 6 months of exposure. Figure 4-15 shows the XRD pattern of the spalled material versus the XRD pattern of the core material at 6 months of exposure.

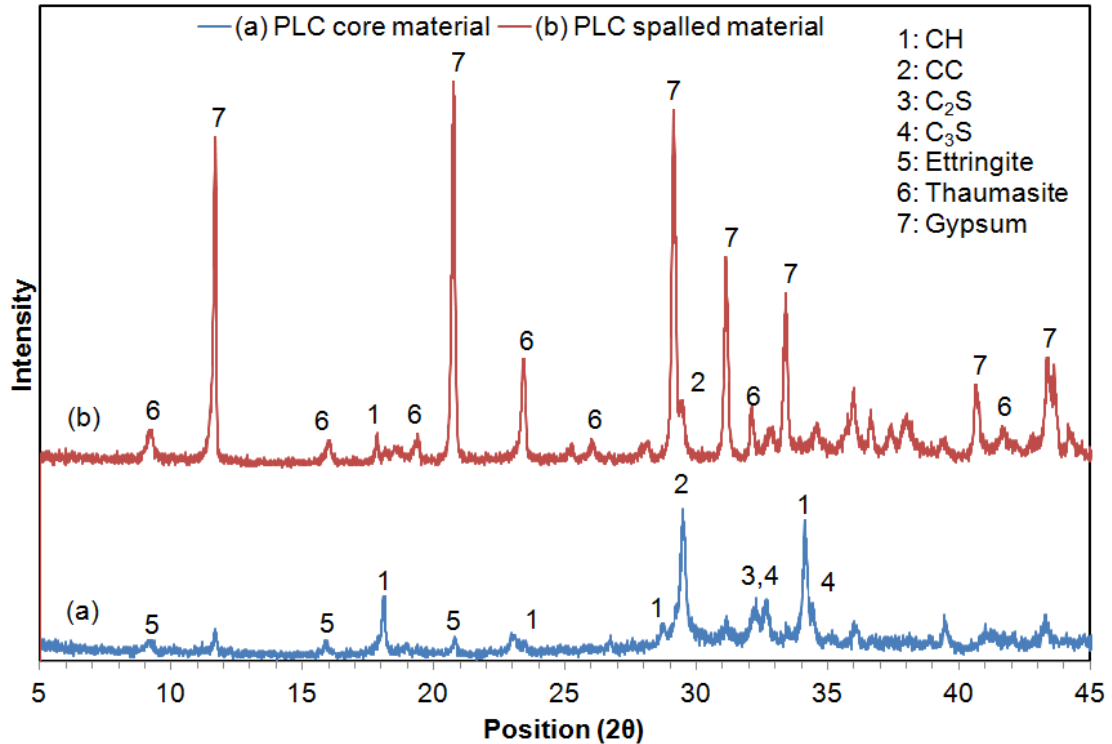


Figure 4-15: XRD patterns of spalled and core of hydrated PLC specimen

As shown in Figure 4-15, there was an important difference in XRD patterns taken from the core and the spalled material. The spalled material, gathered after 6 and 10 months of exposure, showed important peaks corresponding to thaumasite and gypsum. The most pronounced peaks were attributed to gypsum, which indicates that the sulphate attack was well under way. The presence of gypsum has indeed been found to be a characteristic ‘fingerprint’ characterizing external sulphate attack, whether thaumasite or ettringite is being formed (Skalny et al. 2002). The fact that gypsum was dominant in the reaction was attributed to the low pH of the solution (Zhou et al. 2005). Also, the high sulphate concentration could explain the important formation of gypsum. Thaumassite was identified and distinguished from ettringite

due to the presence of characteristic peaks. No thaumasite was identified before the first 6 months of exposure. Also, as shown in Figure 4-15, thaumasite was only present in the spalled material. The mineralogy of the core appeared to be unchanged from earlier patterns (Figure 4-14). This result confirms that thaumasite damage does start at the surface, and progresses inwards of the specimen. The ingress of the sulphates in the specimens then becomes a major factor linked to the deterioration of the specimens. Carbonation could be affecting the ingress. Also noticeable was the important decrease in calcium carbonate peaks between the core and the surface, which can be seen at the major peak at $29^{\circ} 2\theta$ in Figure 4.15. The consumption of calcium carbonates was attributed to the formation of thaumasite.

Finally, Figure 4-16 presents XRD patterns corresponding to carbonated PLC specimens taken throughout the deterioration, from 0 to 10 months of exposure. As no material had spalled during the first 10 months of the exposure period, the powder that was tested was taken from the outer surface of the cement paste cubes, similarly to OPC and COPC.

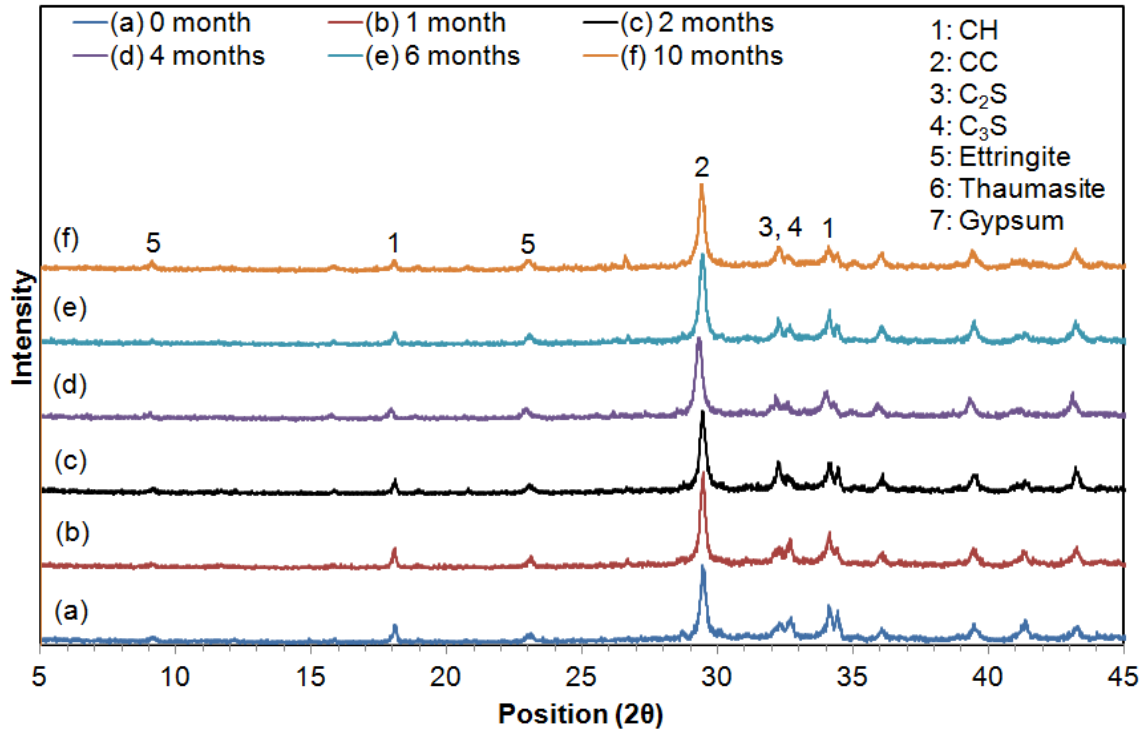


Figure 4-16: XRD patterns of carbonated PLC specimens

Similarly to carbonated OPC, a small peak corresponding to ettringite was found in carbonated specimens at around $9^\circ 2\theta$. However, the peak was present before exposure to the sulphate solution and remained afterwards. No signs of thaumasite, gypsum or other sulphate attack compounds were found. Unlike the hydrated PLC specimens, the pronounced calcium carbonate peaks, due to the combination of carbonation curing and the addition of limestone powder, were not consumed. Therefore, carbonation had a significant impact on the mineralogy, allowing for increased resistance of specimens to TSA.

It was evident from the XRD results that carbonation had improved the cement mineralogy to be more resistant to sulphate attack at low temperatures. As noticed in section 4.2, the difference was especially noticeable between PLC and CPLC. Indeed, spalled PLC specimens showed clear signs of deterioration through the formation of gypsum and thaumasite. From the results presented in this section, it was also possible to conclude that the deterioration was progressing from the surface to the core of the specimens.

4.3.2 Thermogravimetric Analysis (TGA) and Differential Thermal Analysis (DTA)

TGA/DTG and DTA were also used to evaluate the chemical/mineralogical decomposition of cement specimens. The experiments were performed on specimens that had been exposed for 10 months to the sulphate solution at 5°C. For hydrated PLC paste, the analysis was performed on both core and spalled material on the surface. The other three groups of specimens were examined on a surface layer of 2-mm since there was no spalling. DTA was of use as it can lend insight due to an endothermic peak at 206°C that corresponds to thaumasite, which begins between 135 and 140°C, and ends between 255-260°C (Font-Altaba 1960).

TGA/DTG was also used to differentiate the carbonates formed by carbonation to those from limestone filler. Ramachandran and Beaudoin (2001) classified the mass loss along TG curves into 6 categories: evaporable water (up to 105°C), bound water in poorly formed CSH (105°C-200°C), bound water in well-formed CSH and CAH (200°C-420°C), bound water in calcium hydroxide

(420°C-550°C), CO₂ in poorly crystalline or amorphous calcium carbonates (550°C-720°C) and CO₂ in well crystalline calcium carbonates (720°C-950°C). Therefore, the carbonates can be determined by the TG curve from a range of 550 to 950°C.

The DTA results are shown in Figure 4-17. The peak observed in all instances at approximately 150°C, except in the case of spalled PLC, was attributed to the decomposition of bound water. It was seen that the spalled PLC material was affected by thaumasite, which was observable by the mineralogical decomposition. There was a broad endothermic peak ranging from approximately 130°C to 220°C. This peak was attributed to the decomposition of thaumasite, which has an endothermic peak at approximately 130°C (Kakali 2003). The endothermic peak at approximately 820°C in COPC, PLC and CPLC was associated to crystalline calcium carbonates. Therefore, it was possible to confirm the presence of thaumasite using DTA, and reinforce the notion that the spalled PLC material was strongly affected by the deterioration.

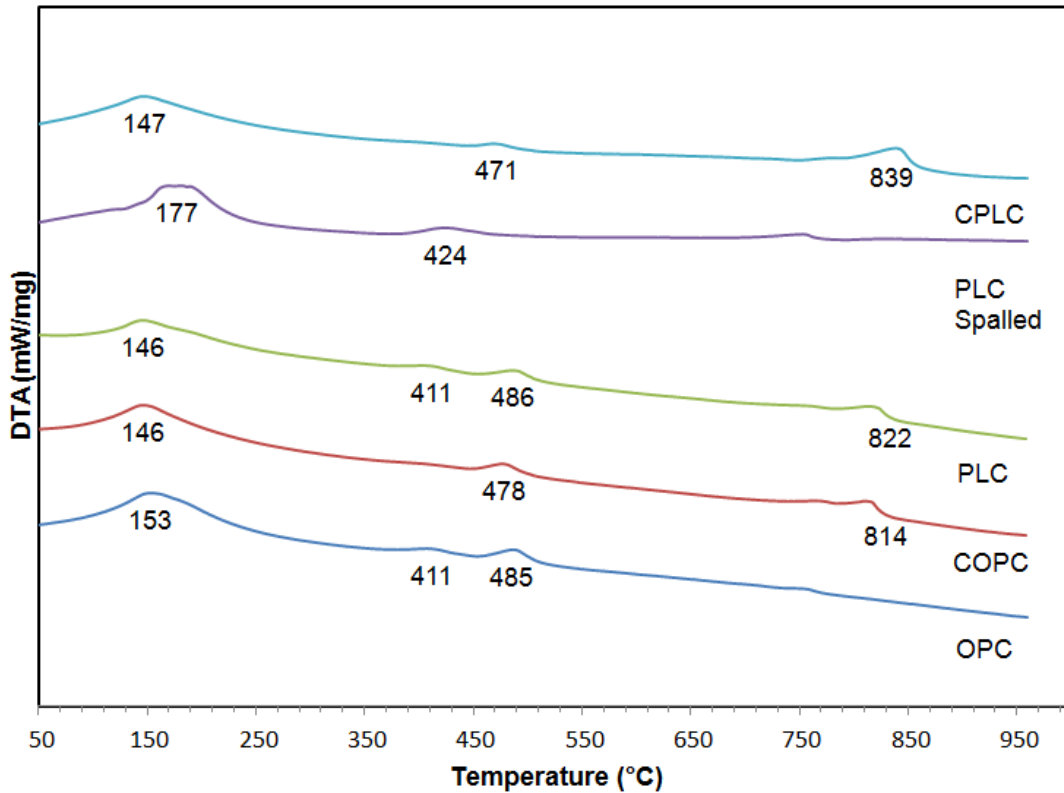


Figure 4-17: DTA of cement pastes at 10 months of $MgSO_4$ exposure

Figure 4-18 shows the DTG results. COPC, PLC core and CPLC showed peaks at approximately 807-834°C that were attributed to highly crystalline carbonates. The peak associated with the decomposition of highly crystalline carbonates was more pronounced in CPLC, due to carbonation curing. Carbonation curing created more highly crystalline carbonates. The crystalline calcium hydroxide peaks were apparent at 479 °C in hydrated cements and at 464-466 °C in carbonated cements. It was noted that the quantity of crystalline CH was reduced in carbonated specimens and the amorphous CH at about 401 – 417 °C was totally consumed by carbonation. The double peak in the range of 158-178 °C in spall material from hydrated PLC was associated the dehydration

of thaumasite and gypsum. The dehydration of ettringite and other hydration products took place at lower temperature between 137 – 145 °C in all cements unaffected by sulphate attack.

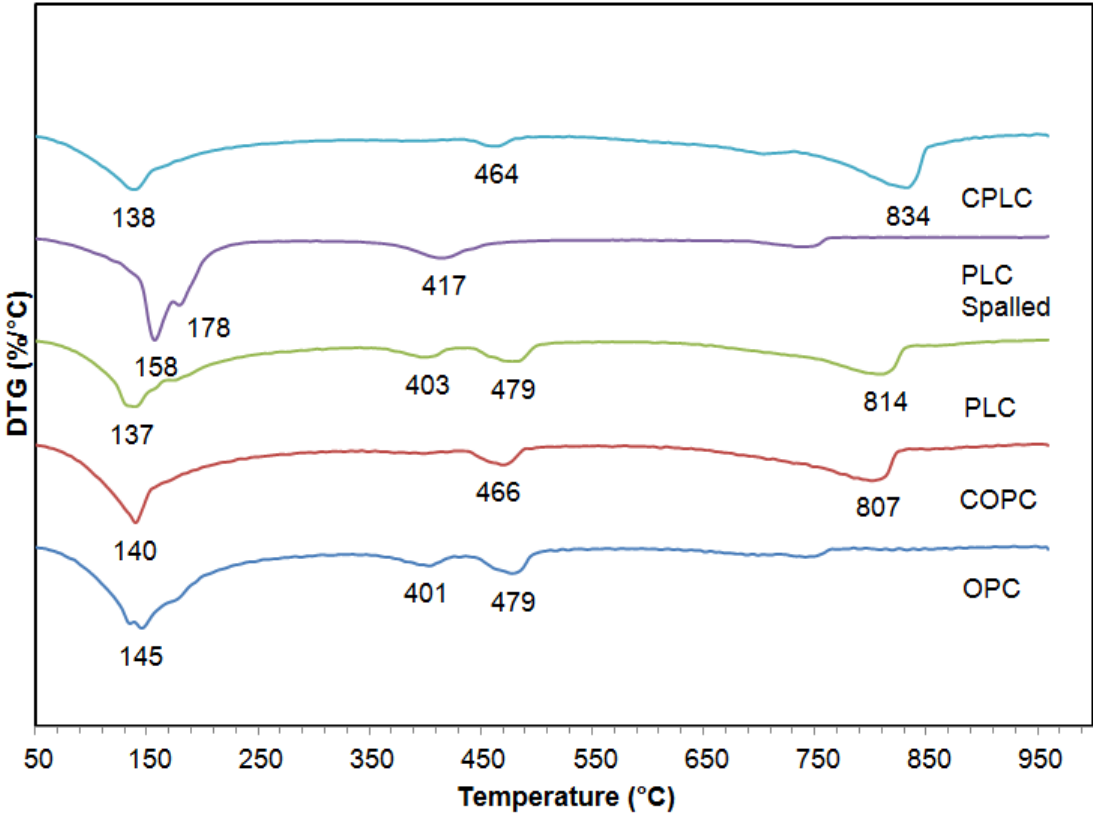


Figure 4-18: DTG of cement pastes at 10 months of MgSO₄ exposure

The quantitative analysis of TG results is shown in Figure 4-19. It was seen that the mass loss from 420-540°C, which represented bound water from crystalline calcium hydroxide, was less in carbonated OPC and PLC pastes. Also, when comparing the spalled and core PLC specimens, the CO₂ loss was much more in the core material than in the spalled material, indicating that calcium carbonates were consumed in the spalled material from the formation of

thaumasite. In the case of carbonated specimens, the value of CO₂ loss was close to CO₂ content determined by carbon analyzer (Table 4-2). It was 6.87% by carbon analyzer versus 8.6% by TG in carbonated OPC, and 11.4% by carbon analyzer versus 12.8% by TG in carbonated PLC. It was noted that the CO₂ content was measured on a surface layer of 2-mm thick in carbonated cements. This result indicated that the carbonates produced from carbonation curing were not consumed, and therefore thaumasite was not formed.

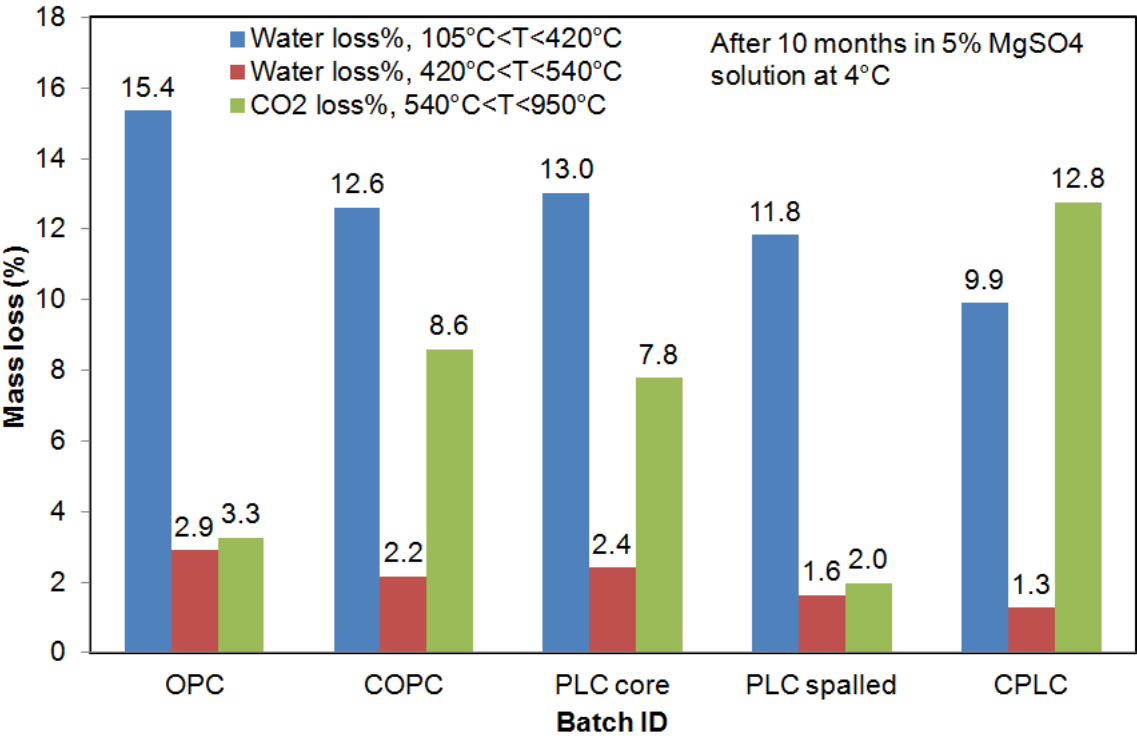


Figure 4-19: Quantitative TG analysis of cement paste at 10 months of MgSO₄ exposure

In conclusion, TGA/DTG and DTA provided more insight into the mineralogical composition of specimens, especially in terms of calcium hydroxide and calcium carbonates. It was possible to confirm the presence of thaumasite

using DTA. Carbonation curing formed highly crystalline carbonates and consumed calcium hydroxide in paste. Also, the fact that the spalled and core material results were different enhanced the notion that the mineralogical composition of the core was not yet affected by TSA. Calcium carbonates of the spalled PLC specimens were consumed due to TSA. Finally, the improved resistance of carbonated specimens was demonstrated by comparing the mineralogical composition of spalled and carbonated PLC. It was also seen that the produced carbonates from carbonation curing were not consumed by TSA.

4.3.3 Raman spectroscopy

The presence of thaumasite and the effect of TSA on the mineralogical composition of cement paste specimens was also assessed using Raman spectroscopy. This type of experiment allows for the identification of thaumasite due to a distinct peak at 658 cm^{-1} , which corresponds to sulfur. The peaks corresponding to thaumasite, gypsum and ettringite are shown in Figure 4-20.

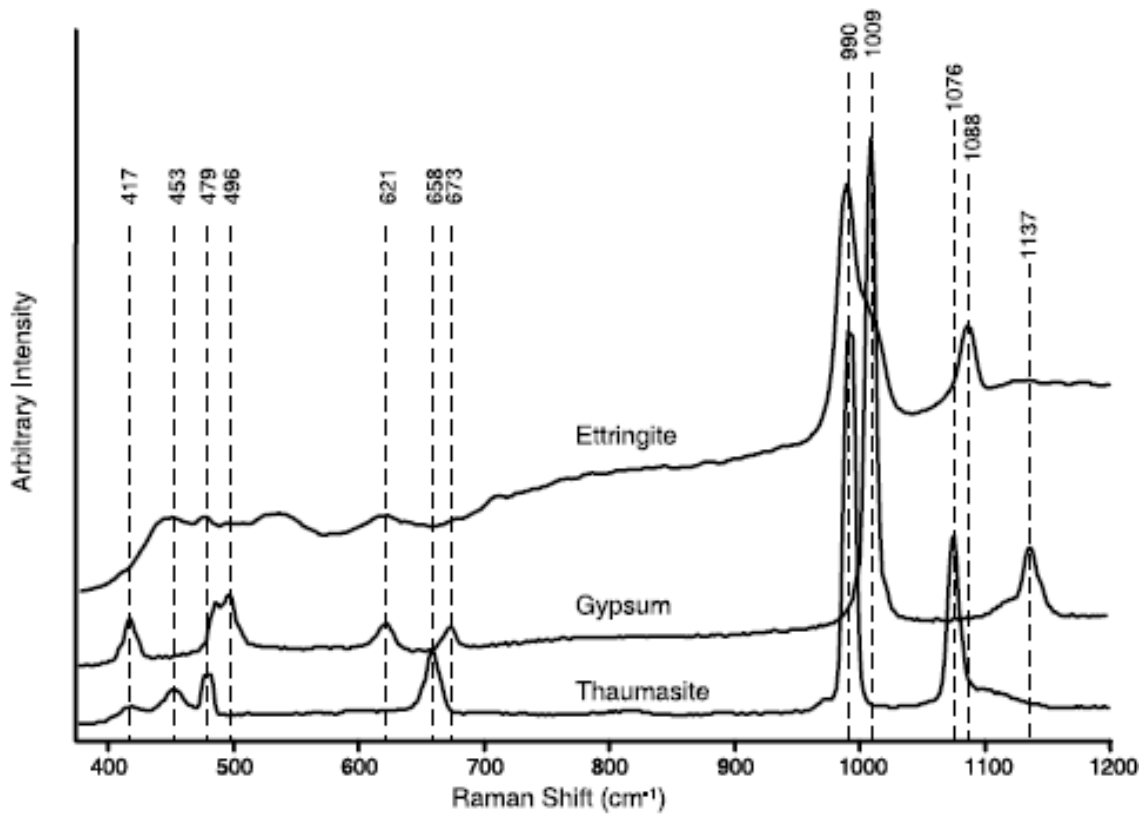


Figure 4-20: Raman spectra of thaumasite, ettringite and gypsum (Sadananda et. al. 2002)

As shown in Figure 4-20, thaumasite has three major peaks at 658, 990, 1076 cm^{-1} and three minor peaks at 417, 453, 479 cm^{-1} . Ettringite has major peaks at 990, 1088 cm^{-1} . Gypsum has a major peak at 1009 cm^{-1} and minor peaks at 417, 496, 621, 673, 1137 cm^{-1} . The presence of thaumasite can therefore be confirmed mainly due the peak at 658 cm^{-1} which corresponds to sulfur. As mentioned previously, the Raman spectroscopy experiment was conducted with powder taken from specimens that had been exposed to 10 months of sulphate attack at 5°C. Similarly to TGA and XRD, Raman spectra were generated for both core and spalled material for hydrated PLC specimens. Other groups of specimens had no spalled material up to 10 months of exposure.

Therefore, powder taken from the outermost layer was used for the experiment, similarly to previous XRD experiments. The Raman spectra of OPC, COPC, PLC core, PLC spalled and CPLC specimens are shown in Figure 4-21.

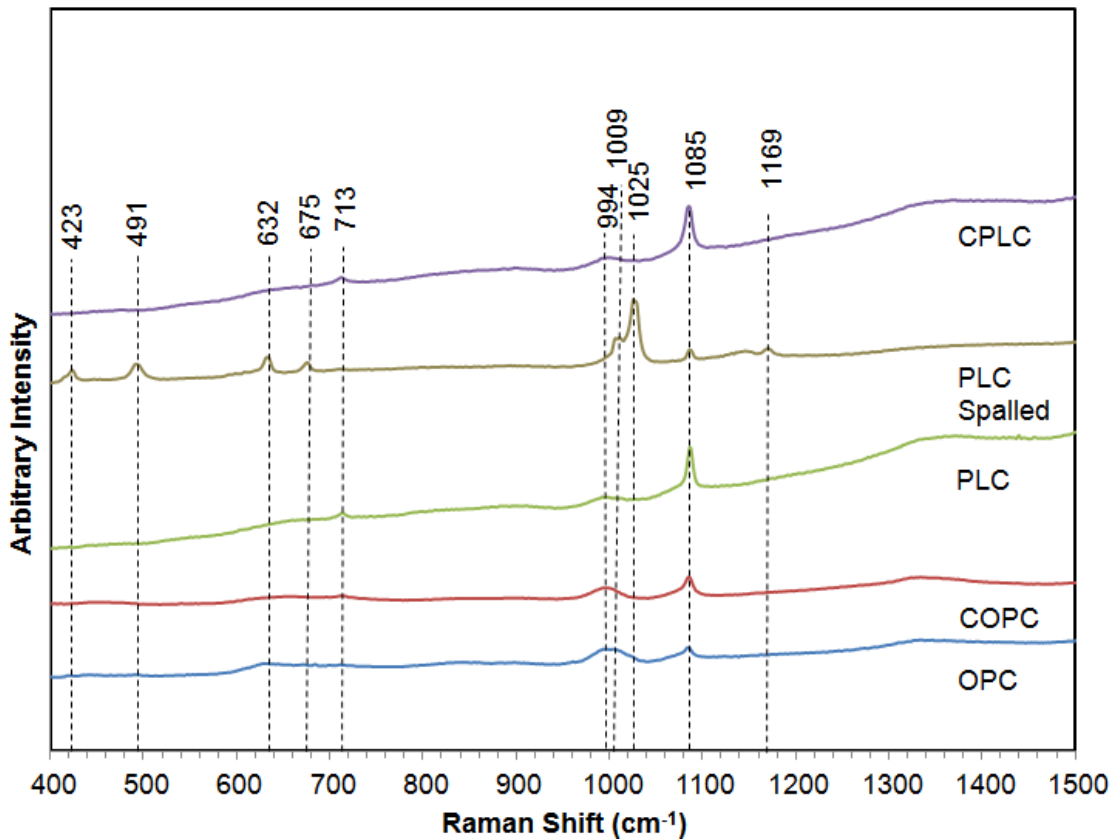


Figure 4-21: Raman spectra of cement paste cubes exposed to sulphate attack for 10 months at 5°C

As shown in Figure 4-21, the spectra corresponding to spalled PLC specimens differed with the spectra obtained from other groups of specimens, including the core of the same PLC specimen. This observation was also made using TGA and XRD. Therefore, from these observations, it was possible to confirm that TSA was progressing from the outer surface to the core, indicating that this was an external form of sulphate attack.

The main peak used to distinguish thaumasite from ettringite and gypsum, located at 658 cm^{-1} , as stated previously, was not seen. It is possible that the amount of thaumasite was not sufficient to be detected using Raman spectroscopy.

Gypsum was identified in spalled PLC specimens due to a peak at 1010 cm^{-1} . Many other peaks were found that were very close to those previously recorded for gypsum. However, these peaks at 423, 491, 632, 1025 and 1169 cm^{-1} corresponded more likely to anhydrite, which has been recorded at 423, 490, 630, 1024 and 1166 cm^{-1} (Chang et al. 1999). This mineral, which is a precursor of gypsum, could also explain the peak recorded in spalled PLC specimens at 1169 cm^{-1} . Therefore, it was likely that the formation of anhydrite is an intermediate step towards the formation of gypsum. From this data, it was concluded that a significant amount of gypsum was being formed through the deterioration reaction, which was attributed to the low pH and high concentration of the magnesium sulphate solution.

A broad peak was found at approximately 994 cm^{-1} in all spectra except the one corresponding to the spalled PLC material. Kirkpatrick et al. (1997) have recorded CSH in the range of $950\text{-}1000\text{ cm}^{-1}$. This finding supports the previous research stating that TSA decalcifies the CSH. The decalcification of CSH could explain the consumption of the CSH peak in the spectra of the spalled material.

The peak recorded at 1085 cm^{-1} was also consumed in the spalled material compared to all other specimens. This peak likely corresponded to

calcium carbonates, which have been previously reported at approximately 1090 cm^{-1} (Bensted 1977). The fact that this peak was consumed in the spectra corresponding to the spalled material confirmed the fact that calcium carbonates were consumed for the formation of thaumasite. This finding was also noticed using both TGA and XRD.

In conclusion, it was not possible to identify thaumasite using Raman spectroscopy. It was however possible to identify gypsum. Anhydrite was also found, which indicates that gypsum was still being formed. From the Raman spectra, it was also possible to notice the consumption of the CSH and calcite, due to the deterioration reaction from TSA. Finally, the difference in mineralogical composition between spalled and core PLC, observed using TGA and XRD, was also noticed in the Raman spectra. This observation confirmed the fact that TSA was progressing from the surface to the core of specimens. This finding confirms that the ingress of sulphates has a significant impact on the deterioration of the specimens in the presence of TSA.

4.4 Mechanism of sulphate resistance by early age carbonation

The results found in sections 4.2 and 4.3 showed that carbonation improved the resistance of cement to TSA. The differences observed between the mineralogical composition of hydrated and carbonated PLC specimens helped confirm this fact. The mechanism of sulphate resistance by early age carbonation is examined in this section. The first portion focuses on the gas permeability properties of the specimens. Another possible explanation to the

improved resistance of carbonated specimens is the nature of the carbonates that are produced during carbonation. Therefore, the second portion discusses the nature of carbonates using the DTG results shown in section 4.3. The pH of the specimens also has an important influence on the formation of thaumasite. The pH of the cement specimens is presented in section 4.3 of Chapter 4. The fourth section discusses the possibility that the improved resistance of carbonated specimens is attributed to the consumption of calcium hydroxide during carbonation.

4.4.1 Surface air permeability

To examine the difference between hydrated and carbonated specimens, surface air permeability was determined. Indeed, XRD results showed that thaumasite was being formed from the surface inwards. These results were validated using TGA, DTA, and Raman spectroscopy. From this information, it was seen that surface permeability played a predominant role in the damage experienced by TSA. Surface air permeability was considered an important indicator that could explain the difference in deterioration and microstructure of the specimens exposed to the sulphate solution. The surface air permeability results are presented in Figure 4-22.

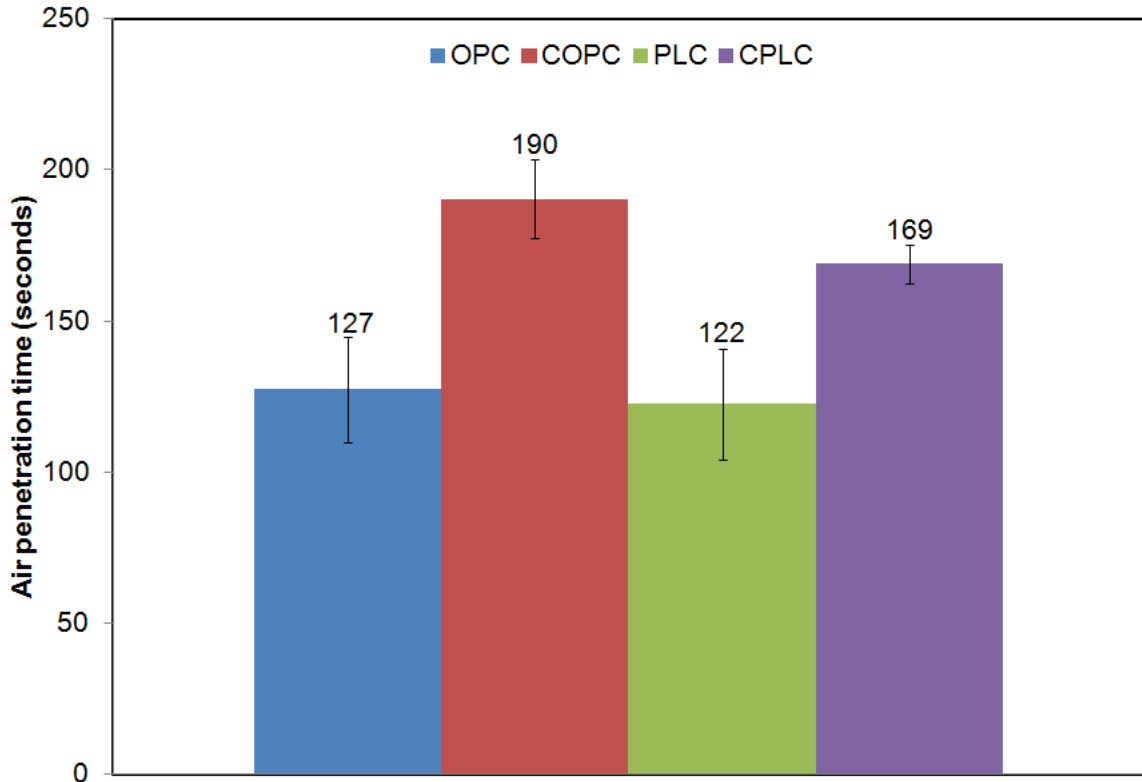


Figure 4-22: Surface air permeability of cement paste specimens

Based on surface permeability test principle, longer the air penetration time represents more resistance to the permeation. The air penetration time showed that the carbonated specimens were more resistant to air permeation than the hydrated specimens. The air penetration time was increased by 50% in carbonated OPC and by 39% increase in carbonated PLC. Both hydrated OPC and PLC showed very similar permeability results. The permeability properties of carbonated specimens could however explain that less damage was caused, especially when comparing PLC specimens. The less permeable outer surface could be attributed to the precipitation of carbonates in the pore structure. Carbonation has proven to lead to the densification of the pore structure due to the precipitation of calcium carbonates during the carbonation reaction. The

outer layer of carbonated specimen, where most of the carbonation reaction occurred, could have been blocking the sulphates from entering the specimens. Therefore, the carbonation process slowed down the ingress of the sulphate ions into the specimen, which in turn stopped the TSA and damage.

4.4.2 Crystalline nature of produced carbonates

Another important factor that could explain the effect of carbonation on TSA is the difference between produced carbonates, from carbonation, and carbonates from limestone filler in cement. It is possible that the produced carbonates had different properties which would not allow them to react to form thaumasite. Alternatively, these carbonates could have formed intermingled with other components of cement, and therefore be unavailable in ion form to react and form thaumasite. However, interestingly, carbonated PLC specimens contained both types of carbonates, i.e. produced carbonates from carbonation and carbonates from limestone filler. Table 4-4 presents the morphology of CaCO_3 in cement pastes. It was determined by TG analysis using a decomposition temperature range of 540-710°C for amorphous CaCO_3 and 710 – 950°C for crystalline CaCO_3 .

Table 4-4: Morphology of CaCO_3 in cement pastes

Batch ID	CaCO_3 content (CA, %)	CaCO_3 content (TG, %)	Amorphous CaCO_3 , (TG, %)	Crystalline CaCO_3 , (TG, %)
OPC	5.0	7.41	3.86	3.55
COPC	15.6	19.55	5.14	14.41
PLC	15.2	17.68	4.41	13.27
CPLC	25.9	29.03	8.05	20.98

Note: CA: by carbon analyzer; TG by thermogravimetric analysis

From Table 4-4, it was possible to conclude that carbonation lead to the formation of highly crystalline carbonates. Hydrated and carbonated OPC had a crystalline CaCO_3 content of approximately 4% and 14% respectively. Carbonated PLC had the highest crystalline CaCO_3 content of 21% and did not suffer any damage, versus 13% for hydrated PLC, which was highly deteriorated. These highly crystalline carbonates may have formed around the carbonates from limestone filler, not allowing the reaction to occur. Also, due to the highly crystalline structure, the carbonates could be unavailable in ion form. However, carbonated OPC had similar crystalline carbonate content as hydrated PLC. Therefore, the crystalline nature of produced calcium carbonates alone does not explain the improved resistance of carbonated specimens to TSA, although it could be one contributing factor.

4.4.3 pH measurements

The pH of the specimens can have an influence on whether or not thaumasite formation will occur. It has been found that the higher the pH, the higher the likelihood of thaumasite being formed (Crammond 2003). The pH of the specimens measured at the outer surface, inner surface and core using a pH meter equipped with a flat sensor head of 9mm in diameter is shown in Figure 4-23.

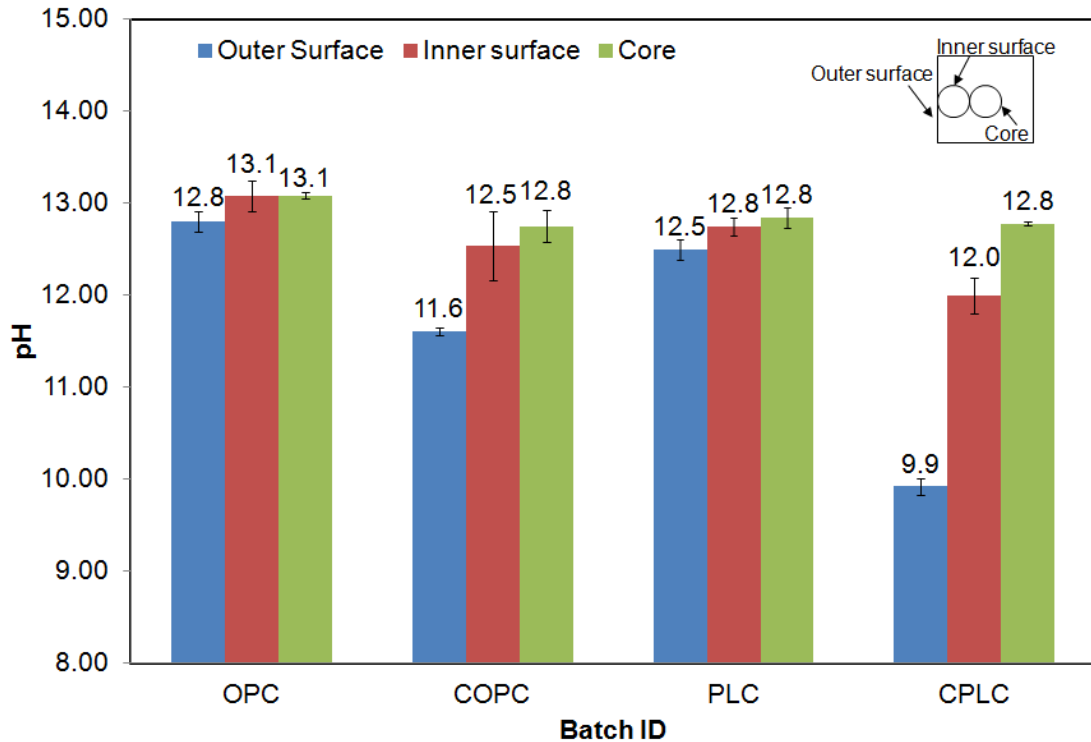
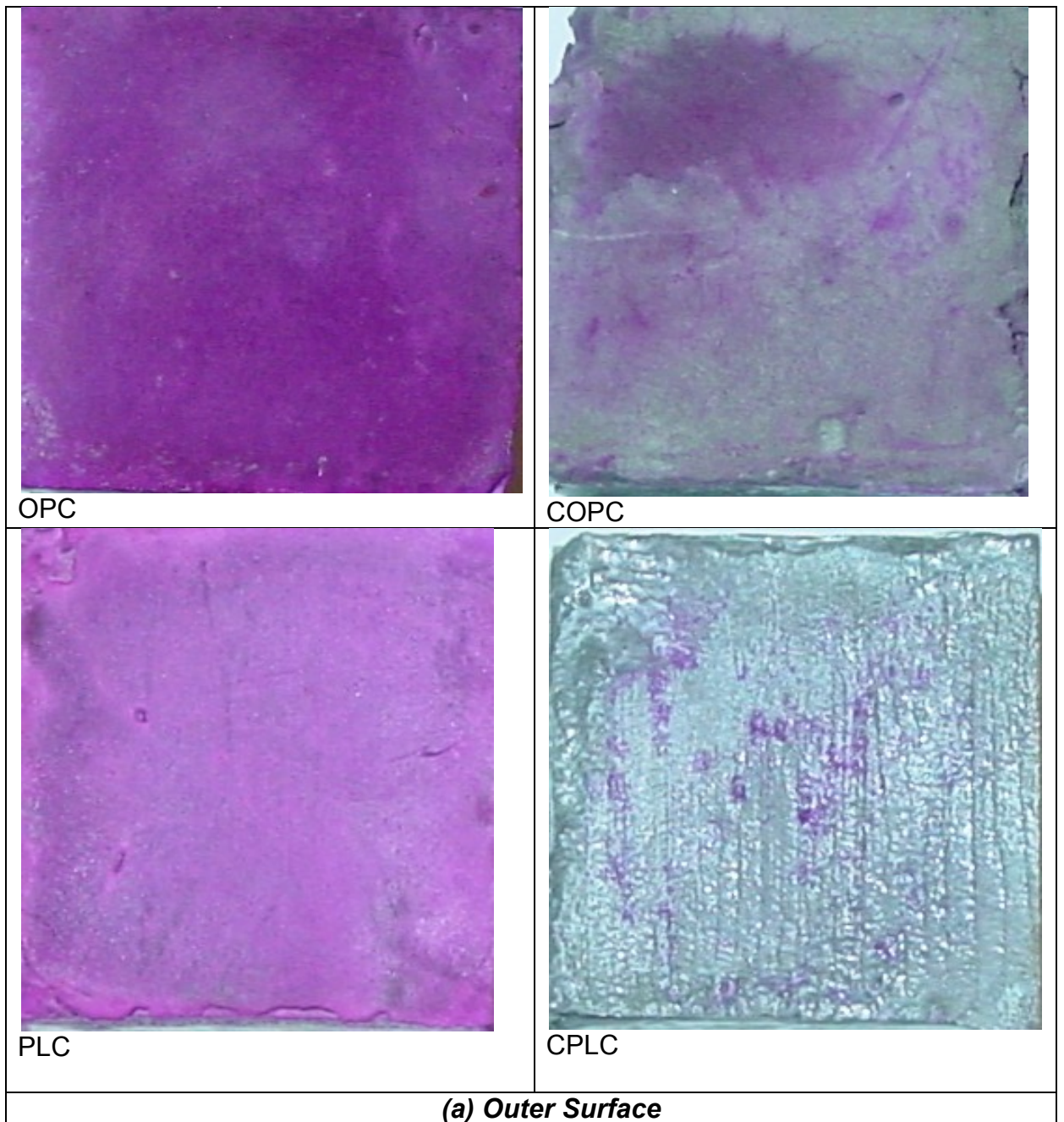


Figure 4-23: pH of cement paste cubes

The results show that carbonation curing had reduced the pH of the surface of cement paste specimens. The reduction in pH was especially noticeable at the outer surface. The pH of the core of carbonated specimens was similar to hydrated specimens, indicating that carbonation had not reached the core, as found earlier. Therefore, the reduction in pH from carbonation curing could have played an important role in improving the resistance of specimens. The change of pH in carbonated specimens was confirmed by spraying phenolphthalein at the outer surface and cross-section of specimens, as shown in Figure 4-24. From the photographs, it was clear that the pH was greatly reduced at the outer surface of carbonated specimens. The difference was less

apparent at the cross-section, but still noticeable when comparing hydrated PLC and carbonated PLC specimens. It was seen that carbonation had not reached the core of specimens. Therefore, the phenolphthalein tests confirmed the pH readings.



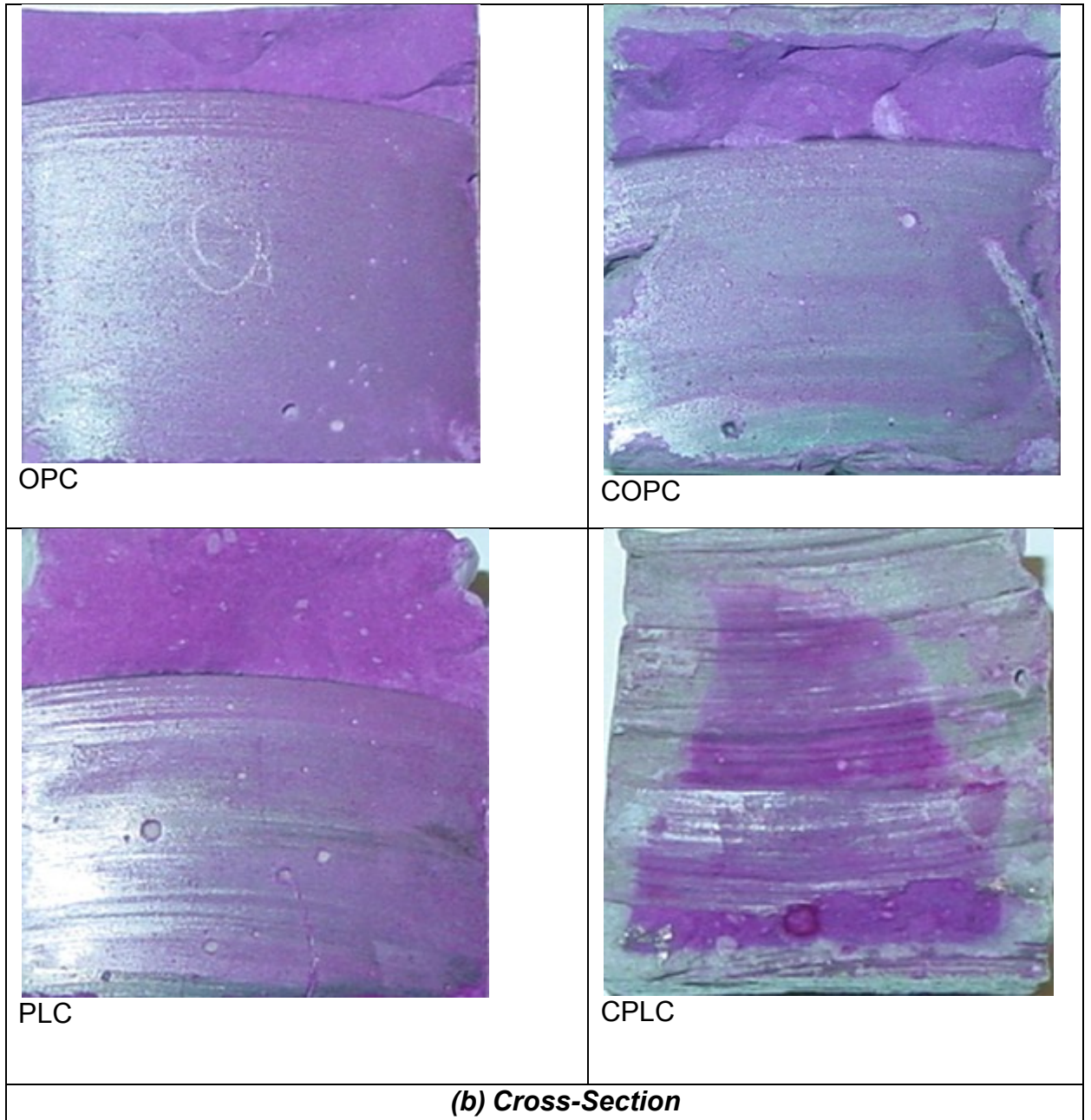


Figure 4-24: Phenolphthalein photographs at the outer surface (a) and cross-section (b) of specimens

4.4.4 Calcium hydroxide content

One of the reactants required for the formation of thaumasite is calcium hydroxide. XRD and TGA results showed that carbonation curing consumed a

portion of calcium hydroxide from the cement paste. Therefore, it is possible that by removing this reactant, the formation of thaumasite was slowed down in carbonated specimens.

From the results presented and discussed in this section, it is possible to conclude that early age carbonation curing had improved cement resistance to TSA by four factors. First, the improved performance was attributed to the improved resistance to surface air permeation, resulting from the densification of the pore structure. As well, the difference in crystalline nature between the carbonates produced, and those initially present in the cement, improved resistance to TSA. Indeed, it was found that carbonation yielded highly crystalline calcium carbonates. Another explanation was the reduced pH that was found in carbonated specimens, which is known to impede the formation of thaumasite. Finally, the fact that calcium hydroxide was consumed during carbonation, which reduced reactants for thaumasite formation, improved the resistance to TSA.

Chapter 5: Conclusions

The objectives of the research presented in this thesis were to perform early age carbonation curing of OPC and PLC pastes, to study the thaumasite form of sulphate attack in carbonated OPC and PLC, and to understand the effect of early age carbonation curing on the formation of thaumasite. This research, where a specimen is cured at an early age using CO₂ and exposed to a TSA-inducing environment, has not been studied in previous research. This work is therefore entirely original, and the results can provide important insight in carbonated concrete durability to TSA. It was concluded that carbonation can considerably improve the resistance of cement paste containing calcium carbonates to TSA.

Deterioration of specimens from TSA was monitored throughout the exposure period. Visually, hydrated specimens suffered more damage than carbonated specimens. This distinction was especially noticeable with PLC specimens. The same trend was seen for mass loss. Mass loss was however found to be an indicator of damage only when the deterioration was strongly advanced, due to the absorptive nature of specimens that cancel out negligible mass loss. Compressive strength was extremely reduced when advanced TSA had taken place in the PLC specimens. Carbonated specimens did not show noticeable loss of compressive strength up to 10 months of exposure. Finally, change in length results also showed that carbonation curing was beneficial. Expansion of hydrated specimens was nearly twice as high as the carbonated. It was also found that OPC specimens suffered the most expansion, which could

be explained by the fact that ettringite was actually being formed in OPC specimens. The formation of ettringite instead of thaumasite was explained by the fact that OPC specimens did not have sufficient carbonate ions from the lesser amount of limestone present in the cement. PLC specimens suffered expansion, but the expansion was less in comparison to OPC mortar bars. This difference in expansion was indicative that expansion alone was not the most representative sign of TSA-induced damage. Indeed, PLC specimens suffered more decalcification damage, but OPC specimens suffered more expansion. The results also confirmed the fact that with an increasing amount of limestone filler, more TSA damage in PLC was observed.

Mineralogical composition/decomposition analysis of specimens was also presented. Phase analysis was conducted throughout the deterioration using XRD. It was shown that PLC specimens formed thaumasite and significant amounts of gypsum after approximately 6 months of exposure to the sulphate solution. OPC specimens formed ettringite, but no thaumasite was found in 10 months of exposure. Carbonated specimens did not have any sulphate attack compounds. Therefore, it was confirmed that carbonation did improve the performance of paste in TSA-inducing environments. It was possible to confirm the presence of thaumasite using DTA, but not using Raman spectroscopy. Nonetheless, by testing both spalled and core PLC specimens, it was confirmed that the reaction progressed from the surface to the core. The Raman spectroscopy results also indicated that the CSH and calcium carbonates were being consumed by TSA in spalled PLC specimens. This finding confirmed the

fact that the formation of thaumasite decalcified the CSH, and consumed calcium carbonates.

From the results, it was found that hydrated OPC did not show thaumasite formation, despite a 5.0% CaCO_3 content. Hydrated PLC, which contained 15.2% limestone, was badly damaged due to TSA. Both carbonated OPC and PLC, which contained 15.6% and 25.9% respectively, did not suffer any damage. To explain the difference in resistance between hydrated and carbonated specimens in terms of physical properties, surface air permeability experiments were performed. It was found that carbonation reduced the gas permeability of the cement paste cubes. TGA was also performed to investigate the crystalline nature of carbonates in hydrated and carbonated specimens. It was found that highly crystalline calcium carbonates were produced during carbonation. These highly crystalline calcium carbonates were not found in hydrated cement. Therefore, the crystalline nature of the carbonates produced could explain the resilience of the specimens to TSA. Another possible explanation to the improved resistance of carbonated specimens was the reduction in pH at the surface of specimens caused by carbonation. Finally, the consumption of calcium hydroxide from early age carbonation curing also explained the improved resistance of carbonated specimens.

In conclusion, the research found that early age carbonation curing improves the performance of paste and mortars exposed to TSA. The improved resistance of carbonated specimens is explained by a denser pore structure leading to less permeable concrete, the crystalline nature of the carbonates

formed during the carbonation curing process, the reduced pH from carbonation and the consumed calcium hydroxide in carbonated specimens. It is also concluded that PLC specimens are more vulnerable to thaumasite, due to the carbonates from limestone filler. Thaumasite can be better detected using XRD. It is evident that early age carbonation curing has improved properties of cement paste in sulphate-rich environments at low temperatures and in the presence of carbonate ions.

References

- Bensted, J. (1977). Raman spectral studies of carbonation phenomena. *Cement and Concrete Research*, 7, 161–164.
- Bensted, J. (1999). Thaumasite - background and nature in deterioration of cements, mortars and concretes. *Cement and Concrete Composites*, 21, 117–121.
- Chang, H., Huang, P.J., & Hou, S.C. (1999). Application of thermo-Raman spectroscopy to study dehydration of $\text{CaSO}_4 \cdot 2\text{H}_2\text{O}$ and $\text{CaSO}_4 \cdot 0.5\text{H}_2\text{O}$. *Materials Chemistry and Physics*, 58, 12-19.
- Colleparidi, M. (2003). A State-of-the-Art Review on Delayed Ettringite Attack on Concrete. *Cement & Concrete Composites*, 25, 401-407.
- Crammond, N.J. (2003). The thaumasite form of sulfate attack in the UK. *Cement and Concrete Composites*, 27, 809–818.
- Downs, R. T. (2006). The RRUFF Project: an integrated study of the chemistry, crystallography, Raman and infrared spectroscopy of minerals. *Program and Abstracts of the 19th General Meeting of the International Mineralogical Association in Kobe, Japan*.
- Font-Altaba, M. (1960). A thermal study of thaumasite. *Mineralogical Magazine*, 25, 567-572.

- Hartshorn, S.A., Sharp, J.H., & Swamy, R.N. (1999). Thaumasite formation in Portland-limestone cement pastes. *Cement Concrete Research*, 29, 1331–1340.
- Hewlett, P. C. (2004). *Lea's Chemistry on Cement and Concrete*. 4th ed., Elsevier Ltd., Oxford.
- Irassar, E. F. (2009). Sulfate attack on cementitious materials containing limestone filler. *Cement and Concrete Research*, 39, 241–254.
- Kakali G., Tsivilis, S., Skaropoulou, A., Sharp J.H., & Swamy, R. N. (2003). Parameters affecting thaumasite formation in limestone cement mortar. *Cement Concrete Composites*, 25, 977–981.
- Kirkpatrick, R. J., Yarger, J.L., McMillan, P. F., Yu, P., & Cong X. (1997). Raman spectroscopy of C-S-H, Tobermorite, and Jennite. *Advanced Cement Based Materials*, 5, 93-99.
- Neville, A. (2004). The confused world of sulfate attack on concrete. *Cement and Concrete Research*, 34, 1275–1296.
- Ramachandran, V. S., & Beaudoin, J. J. (2001). Handbook of Analytical Techniques in Concrete Science and Technology. *William Andre Publishing/Notes*.
- Rostami, V., Shao, Y. Boyd, A.J., & He, Z. (2012). Microstructure of cement paste subject to early age carbonation curing. *Cement and Concrete Research*, 42, 186-193.

- Sadananda, S., Exline D. L., & Nelson, M. P. (2002). Identification of thaumasite in concrete by Raman chemical imaging. *Cement and Concrete Composites*, 24, 347-350.
- Santhanam, M., Cohen, M. D., & Olek J. (2003). Effects of gypsum formation on the performance of cement mortars during external sulfate attack. *Cement and Concrete Research*, 33, 325-332.
- Shao, Y., Mirza, M. S., & Wu, X. (2006). CO₂ sequestration using calcium-silicate concrete. *Canadian Journal of Civil Engineering*, 33, 776-784.
- Skalny, J., Marchand, J., & Odler, I. (2002). Sulfate Attack on Concrete. *Modern Concrete Technology Series*, Spon Press, London.
- Skalny, J., & Pierce, J.S. (1999). Sulfate Attack Issues: An Overview, in: Materials Science of Concrete: Sulfate Attack Mechanisms, J. Marchand and J. Skalny eds., *American Ceramic Society*, 49-63.
- Tennis, P.D., Thomas, M.D.A., & Weiss, W.J. (2011). State-of-the-art report of use of limestone in cements of up to 15%. *Portland Cement Association*.
- Tian, B., & Cohen, M.D. (2000). Does Gypsum Formation During Sulfate Attack on Concrete Lead to Expansion? *Cement and Concrete Research*, 30, 117–123.
- Torres, S.M., Kirk, C.A., Lynsdale, C.J., Swamy, R.N., & Sharp, J.H. (2004). Thaumasite–ettringite solid solutions in degraded mortars. *Cement and Concrete Research*, 34, 1297–1305.

Tsivilis, S., Sotiriadis, K., & Skaropoulou, A. (2007). Thaumaside form of sulphate attack (TSA) in limestone cement pastes. *Journal of the European Ceramic Society*, 27, 1711-1714.

Zhou, Q., Hill, J., Byars, E.A., Cripps, J.C., Lynsdale, C.J., Sharp, J. H. (2006). The role of pH in thaumasite sulfate attack. *Cement and Concrete Research*, 36, 160-170.